

# An integrated approach to the study of intramolecular hydrogen bonds in malonaldehyde enol derivatives and naphthazarin: trend in energetic versus geometrical consequences

Ryza N. Musin and Yitbarek H. Mariam\*

Department of Chemistry and Center for Theoretical Studies of Physical Systems, Clark Atlanta University, Atlanta, Georgia 30314

Received 18 November 2005; revised 4 May 2006; accepted 26 May 2006



**ABSTRACT:** Density functional and atoms-in-molecules (AIM) and natural bond orbital (NBO) approaches have been applied in the study of energetic (**E**), geometrical (**G**) and electronic (AIM and NBO) consequences of H bonding in malonaldehyde (MAE) derivatives and naphthazarin (NZ). AIM parameters and other measures of HB strength were used: (a) for the verification of (i) the reliability of the O...O distance (**G** consequence) as an indicator of IMHB strength; (ii) the capacity of the classically computed energetic parameters ( $\Delta E_{\text{SES}}$ ) to serve as acceptable measures of IMHB strength; and (b) for the separation of the  $\Delta E_{\text{SES}}$  into (i) stabilization (HB) energies ( $E_{\text{HSE}}$ ) that serve as apparent IMHB energies ( $E_{\text{HB,AS}}$ ), and (ii) stabilization (isomerization) energies ( $E_{\text{NSE}}$ ) that do not (owing to intractable contributions that are not germane to the solitary HB donor(D)-acceptor(A) interactions). Some of the sources of the anomalies have been rationalized. AIM topological properties were used to study the nature of the IMHB interactions. An exponential parametric model for the correlation of  $E_{\text{HSE}}$  with the O...O distance, which has asymptotic characteristics at long O...O distances, was obtained. The model (a) has predictive ability, that is, can be used to estimate, in an empirical manner,  $E_{\text{HB,AS}}$  that are otherwise grossly underestimated, and (b) can treat both the MAE derivatives and the NZ systems even though they possess very different resonant spacers connecting the HB D-A segments. MAE and NZ are also demonstrated to have essentially the same IMHB strength. By contrast, a quadratic model for  $E_{\text{HSE}}$ -HB distance correlation was found to be unphysical. Use of electronic consequences of H bonding was shown to be essential for study of IMHBs with intractable interactions. Thus, AIM energy density and NBO second-order interaction energy parameters were used for the verification of predictions of IMHB strengths made on the bases of energetic and geometrical consequences. Copyright © 2006 John Wiley & Sons, Ltd.

*Supplementary electronic material for this paper is available in Wiley InterScience at <http://www.interscience.wiley.com/jpages/0894-3230/suppmat/>*

**KEYWORDS:** intramolecular hydrogen bonding; malonaldehyde enol; naphthazarin; dihydroxynaphthoquinone; resonance-assisted hydrogen bonds; intractable interactions; energetic, geometrical, and electronic consequences; atoms in molecules (AIM); natural bond orbital (NBO)

## INTRODUCTION

Hydrogen bonds (HBs) play major roles in influencing the structure and behavior of organic and inorganic compounds and biomolecules, in molecular processes, and in chemical reactivity.<sup>1–9</sup> Hydrogen (H) bonding may also play important roles in the biomedical activity of some drugs. Of particular interest to this work in this regard is the case of the anthracyclines daunomycin (DN) and adriamycin (AD), which are very effective anti-tumor

agents, but whose anti-tumor efficacy has been plagued by dose-dependent cardiotoxic side effects.<sup>10</sup> 5-imino-daunomycin (5IDN), the iminoquinone derivative of DN,<sup>11,12</sup> seems to be, however, devoid of the aforementioned side effects.<sup>11,13</sup> In an attempt to provide with an explanation for the observed difference in this critical biochemical reactivity, differences in the H bonding properties of DN/AD versus that of 5IDN have been invoked as one of the possible reasons.<sup>11,13</sup> However, the nature of the intramolecular HBs (IMHBs) in the aforementioned drug molecules is not completely understood yet.<sup>14</sup>

The H-bonded segments of the pharmacophores of AD and DN include dihydroxynaphthoquinone (otherwise known as naphthazarin (NZ), Chart 1). Hence, NZ may be used to model the H bonding properties of AD and DN. NZ, in turn, consists of the six-membered cyclic

\*Correspondence to: Y. H. Mariam, Department of Chemistry, Clark Atlanta University, Atlanta, GA, 30314, USA.

E-mail: ymariam@cau.edu

Contract/grant sponsor: HHS/MBRS/SCORE Program; contract/grant number: S06-GM08247.

Contract/grant sponsor: NSF/MRCE; contract/grant number: HRD-915407.

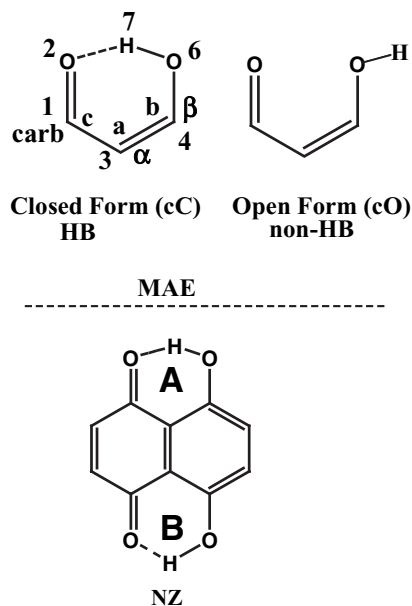


**Chart 1.** Malonaldehyde enol (MAE) in two chemically different environments: the H-bonded (HB) cC and non-H-bonded (non-HB) cO forms. Also shown is dihydroxynaphthoquinone (NZ), with the two H-bonded fragments A and B

HO—C=C—C=O fragments, which are structurally related to the  $\beta$ -diketones malonaldehyde enol (MAE) and acetylacetone enol (AAE). The H-bonding properties of MAE and AAE, which have been attributed to be, in large measure, due to *resonance-assisted H-bonding*<sup>16,17</sup> have been studied extensively.<sup>15</sup> The resonant spacers joining the H-bonded segments in MAE and AAE, and in NZ are however very different (see Chart 1).<sup>18,19</sup> Hence, it cannot be presumed that conclusions emerging from the study of the H bonding properties in MAE and its derivatives (sometimes referred to as *class I systems* henceforth) can be of direct bases to characterize the H bonding properties in NZ and in its tautomers and rotamers thereof (sometimes referred to as *class II systems* henceforth). It is, therefore, of interest to establish the qualitative and quantitative similarities and differences that may exist between the H bonding properties of the two classes of systems.

Unlike in the case of intermolecular HBs,<sup>2,20</sup> a consensus on the nature of the correlation between the energetic (**E**) consequences and the geometrical (**G**) descriptors (such as O...O and O...H distances and O—H bond elongation) of H bonding has not emerged yet in the case of IMHBs. In fact, a cursory review<sup>21</sup> of some of the relevant literature would show contrasting conclusions and disparate observations have been reported<sup>21–28</sup> when it comes to the nature of the IMHB **E**  $\leftrightarrow$  **G** relationship (See Refs. 21 and 25 for details). In one of such reports, Korth *et al.*<sup>27</sup> have pointed out that a primary reason for the lack of **E**  $\leftrightarrow$  **G** correlation for the systems they investigated to be the inability to separate out intractable interactions (that alter the stabilization energies (SEs)) from the sole HB

donor–acceptor interactions. As the result, Korth *et al.*<sup>27</sup> concluded that any attempt to carry out **E**  $\leftrightarrow$  **G** correlations for IMHB cases may not likely succeed.<sup>28</sup> In line with the above, as will be evident in the ensuing sections (*vide infra*), there are also some unresolved issues when it comes to the H bonding consequences in some MAE derivatives. Hence, the nature of the H bonding in some MAE derivatives is not well understood yet either. A reappraisal of some aspects of the previous studies on (a) the MAE derivatives (*vide infra*), and (b) NZ<sup>14</sup> (including the re-evaluation of the estimates for the energies of HB formation reported by us on NZ<sup>14</sup>) is therefore needed. The results to be obtained from such studies are not only important on their own right, but they are also essential for the modeling and understanding of the H bonding properties of the aforementioned drug molecules.

In light of the considerations and motivations briefly discussed above, the specific aims this paper is concerned with are threefold. The first aim is concerned with the establishment of the behavior of the **E**  $\leftrightarrow$  **G** correlation in MAE derivatives. As part of this aim, we plan to determine whether (i) the **E**  $\leftrightarrow$  **G** correlation sought would be in harmony with the behavior observed for intermolecular cases (including the manifestation of asymptotic behavior at long O...O or O...H distances)—otherwise the model might be unphysical, and hence it should be scrutinized properly, and (ii) the model sought would have predictive ability. In the second aim, we seek to (i) establish the similarity and/or difference in the IMHB strengths of MAE and NZ, and (ii) determine if the two classes of systems will be governed by the same **E**  $\leftrightarrow$  **G** correlation.

The use of quantum chemical (QC) calculations alone is not always adequate to compute the energy of intramolecular HB formation (*vide infra*). Hence, the third, and method-oriented, goal of this paper is to assess the advantages of the combined use of QC calculations with either (or both) of the atoms-in-molecules (AIM)<sup>29</sup> or the natural bond orbital (NBO)<sup>30</sup> approaches for the purposes of calibration of the strengths of the H bonding interactions (in those cases when intractable interactions are encountered), along with experimental results when available. Furthermore, we intend to use AIM interaction energy density and other parameters to get insight into the nature of the HB interactions.

## METHODS AND COMPUTATIONAL DETAILS

### Choice of theoretical model and calculations

The B3LYP/6-311G(d,p) model<sup>31</sup> was chosen as the primary method for the present work, because the model has been shown to give good results<sup>32–45</sup> especially for the types of systems to be investigated in this work (See Ref. 32 for details)—additional justification is also provided

in the Results section under Model Chemistry. Some calculations at the B3LYP/6-311++G(d,p), B3LYP/6-311++G(2df,2p), and MP2/6-311++G(d,p) levels have also been done on selected systems as benchmark calculations. Default options of the G98<sup>46</sup> suite of programs were used unless specified otherwise. To a limited extent, the Spartan program was also used.<sup>47</sup> In all cases, frequency (harmonic) calculations have been performed, and zero point energy (ZPE) corrections have been made. AIM topological analyses were carried out in accordance with Bader's approach<sup>29,48–51</sup> using AIM2000<sup>52a</sup> and/or AIMPAC.<sup>52b</sup> DENSITY = CURRENT option was used to generate the wavefunction files (for topological analyses). NBO calculations (at the B3LYP/6-311++G(d,p) level) were carried out using the NBO module (version 3.1) included in G98.

### Calculation of IMHB stabilization energy

Estimates of IMHB SEs ( $\Delta E_{SE}$ ) were obtained as the difference ( $\Delta E_{SE}$ ) between the energies of the equilibrium geometries of the H-bonded (cC form) and non-H-bonded (cO form) conformers defined in Chart 1, that is, via Eqn (1). This approach has been the

$$\Delta E_{SE} = E^{cC} - E^{cO} = E^{HB} - E^{non-HB} \quad (1)$$

standard way for the calculation of intramolecular 'HB energies.' However, the  $\Delta E_{SE}$ s calculated by Eqn (1) may fall into one of two categories: (1) HB SEs that can serve as acceptable indicators of the strengths of IMHBs<sup>26,53</sup> (designated by  $E_{HSE}$  hereafter), and (2) stabilization or conformational energies that do not serve as acceptable indicators of the HB strengths (owing to contributions to  $\Delta E_{SE}$  from intractable interactions that cannot be separated out from the sole HB donor–acceptor interactions).<sup>27</sup> The latter category will be designated by  $E_{NSE}$  hereafter (see Chart 2 for a schematic representation).

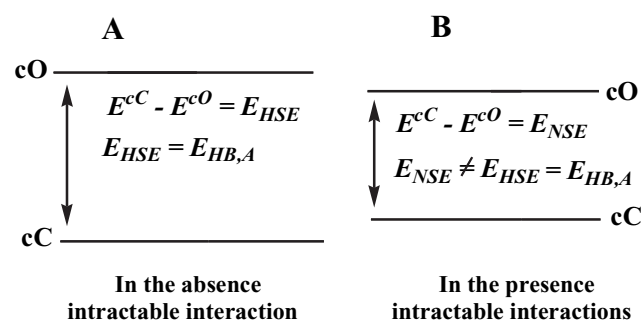


**Chart 2.** A: Hypothetical case when the energy difference,  $\Delta E_{SE}$ , between that of the cC and cO forms is an acceptable measure of the HB SE,  $E_{HSE}$ , and is equal to the apparent HB energy,  $E_{HB,A}$ . B: The energy difference  $E_{NSE}$  that may obtain in the presence of appreciable intractable interactions (that do not contribute to the sole HB interaction). Hence,  $E_{NSE}$  is no longer a measure of the HB strength because  $E_{NSE} \neq E_{HSE} = E_{HB,A}$ .

A priori, it is not possible to determine if a given  $\Delta E_{SE}$  value would belong to one or the other category. Such a determination (as will be done in this report) is therefore necessary. Furthermore, a given  $E_{HSE}$  value is *not a genuine HB energy in the sense the intermolecular HB interaction energy is as given in Refs. [2,54]*. To emphasize this distinction, the  $E_{HSE}$  values—even if they may generally be reasonable estimates of the HB energy<sup>23,55–57</sup>—are referred to in this report as *apparent HB energies*,  $E_{HB,A,S}$ , as opposed to 'HB energies.' Hence,  $E_{HSE} = E_{HB,A}$ , but  $E_{NSE} \neq E_{HB,A}$ .

## SYSTEMS INVESTIGATED AND MODEL CHEMISTRY

### Systems investigated

The systems investigated in this work are divided into classes I and II. The class I systems are further subdivided, for the purposes of discussion, into subclasses IA (consisting of homonuclear —O—H···O=C— IMHB motifs), and IB (consisting heteronuclear IMHB motifs) as shown in Chart 3. Included in subclass IA are the CH<sub>3</sub>, F, and Cl derivatives, and systems **IV** and **V** (Chart 3). Of the subclass IB systems, **VI** and **VII** (with S—H···O and Se—H···O HB motifs, respectively) and **VIII–XII** (with N—H···O HB motifs) are identified, respectively, as subclass IB1 and subclass IB2 (Chart 3). The class II systems include NZ and its tautomer (and their rotamers), which possess two H-bonded segments (A and B, Chart 1). However, in this report results will be presented only for NZ (Chart 1) due to space limitation. Hence, a full report on the class II systems is relegated to a future communication. Some studies have also been done on nitromalonamide (NMA) and benzoylacetone (BAA) (Chart 3).

### Model chemistry

The extent to which both the structural and energetic parameters obtained by the B3LYP/6-311G(d,p) model are reliable can be tested by comparing the results both with experimental data available, and with results obtained from correlated methods such as MP2. Table 1 shows the MP2/6-311++G(d,p) HB binding energies are consistently lower, the average deviation of the B3LYP/6-311G(d,p) and B3LYP/6-311++G(d,p) results being (respectively) about 1.6 and 0.8 kcal/mol (Table 1). Experimental binding energy data are available for **I** (MAE) and **Ibc** (AAE), the values being  $-12.5$  kcal/mol for **I**,<sup>1b,17a</sup> and the estimates ranging from  $-10$  to  $-16.5$  kcal/mol for **Ibc**,<sup>15g,16b,58</sup> that is, the experimental values for **Ibc** are less definitive. Apparently, both the B3LYP and MP2 results are only with modest agreement with the experimental results. The HB strength in **Ibc**



**Table 1.** Comparison of  $\Delta E_{SE}$  values obtained from B3LYP and MP2 calculations<sup>a</sup>

Molecular systems	O...O (Å)	O...H (Å)	B3LYP <sup>b,c</sup>		MP2 <sup>b,d</sup>	MP2 (B3LYP) <sup>e</sup>
			6-311G(d,p)	6-311++G(d,p)	6-311++G(d,p)	6-31G(d,p)
<b>I</b>	2.584	1.686	-13.3	-12.3 (-12.5)	-11.4	-14 (-15)
<b>Ia</b>	2.561	1.659	-13.4	-12.5	-11.9	
<b>Ib</b>	2.561	1.649	-15.4	-14.2	-12.8	
<b>Ic</b>	2.569	1.667	-14.4	-13.5	-12.4	
<b>Ibc</b>	2.549	1.633	-16.2	-15.4 (-10 to -16.5)	-14.6	-16.2 (-17.4)
<b>Iia</b>	2.649	1.777	-10.9	-10.1	-8.8	
<b>Iib</b>	2.436	1.441	-14.5	-13.6	-13.5	
<b>Iic</b>	2.677	1.823	-10.1	-9.2	-8.4	
<b>IIa</b>	2.602	1.717	-12.1	-11.2	-10	
<b>IIb</b>	2.492	1.539	-13.4	-12.6	-11.8	
<b>IIc</b>	2.651	1.792	-9.3	-8.8	-8.5	

<sup>a</sup> O...O and O...H distances are from MP2/6-311++G(d,p) calculations. All energies ( $\Delta E_{SE}$ 's) are in kcal/mol.

<sup>b</sup> This work.

<sup>c</sup> Values in parentheses for **I** and **Ibc** are experimental values.

<sup>d</sup> The MP2 results have some error because the open forms had imaginary low frequencies ( $<200$  with most  $<150\text{ cm}^{-1}$ ) which have been ignored (the imaginary low frequencies seem to arise from methyl torsions (coupled with other motions) in the case of the methyl derivatives, and because the open forms behave as floppy rings). [That the values of the ZPE are based on a harmonic model (in all cases) should also be taken into consideration with regard to the accuracy of the results.]

<sup>e</sup> From Ref. 53b. Values in parentheses are B3LYP results.

As alluded to before, the re-appraisal and comparison of the class II systems with the class I systems is an important aim of the present work. Thus, the use of B3LYP/6-311G(d,p) model was also deemed necessary for the purposes of consistency with previous work on the class II systems.<sup>14</sup> Finally, because our primary interest in this work is to look for trends, the B3LYP/6-311G(d,p) model should be adequate. This view is very consistent with similar conclusions reached at by others in work on IMHBs using the B3LYP method with even a smaller basis set (6-31G(d)) than used here.<sup>27,62</sup> Rabuck and Scuseria<sup>62f,g</sup> have also shown that B3LYP/6-311++G(d,p) is well suited to obtain geometries and energies in hydrogen bonded structures. The B3LYP/6-311G(d,p) results will therefore be used for the analysis to be carried out henceforth. However, *a proviso* to refine the IMHB energetic parameters (to be predicted in an empirical manner) will be made so that they are more in line with the MP2/6-311++G(d,p) results.

## RESULTS AND ANALYSES

### Prefatory calibration of the energetic and geometrical parameters

Given in Table 2 are (i)  $\Delta E_{SES}$ ; (ii) O...X distances,  $R(\text{O}\cdots\text{X})$  (for the cC forms, with X = O, N, S, Se); (iii) O...H HB distances,  $R(\text{O}\cdots\text{H})$ ; (iv) equilibrium X—H bond distances,  $R(\text{X—H})$ , (for the cC forms); (v) Q symmetry coordinate parameters<sup>17</sup> (for subclass IA), and (vi) electron densities,  $\rho_{b,\text{X—H}}$ , at the X—H bond critical points (BCPs) for all the class I systems.

Use of the energetic ( $\Delta E_{SE}$ ) and geometrical (O...O distances) parameters of the systems with O...H—O HB motifs (Table 2) leads to the following tentative rankings in HB strength, respectively, R(E) and R(G):

- R(E): **Ibc** > **Ib** > **IIb** ~ **Ic** > **Ia** ~ **IIb** > **I** > **IIa** > **IV** ~ **IIa** > **IIc** ~ **IIac** > **IIIc** > **V** > **IIbc** > **IIac** > **IIIbc**.
- R(G): **IIb** > **IIIb** > **Ibc** > **V** > **Ib** > **Ic** > **Ia** > **I** > **IIa** > **IIIbc** ~ **IIac** > **IIbc** > **IIa** > **IV** > **IIIc** > **IIc** > **IIac**.

Two of the different classifications of HB strengths that are most discussed in conjunction with intramolecular RAHBs<sup>17c</sup> are those based on the (a) energetic<sup>63</sup> and (b) geometrical (O...O distance)<sup>17c,64</sup> consequences of H bonding, as provided below.

Classification basis	Weak	Strong	Very strong
Energetic (kcal/mol) <sup>63</sup>	2–12	12–24	>24
Geometrical (Å) <sup>17c,64</sup>	$2.5 \leq R(\text{O}\cdots\text{O}) \leq 2.65$		$R(\text{O}\cdots\text{O}) \leq 2.5$

We will thus use these classifications for a preliminary exposition of some of the glaring discrepancies between the above R(E) and R(G) rankings. Because the O...O (and O...H) distances in **IIb** and **IIIb** are shorter than the corresponding distances in **Ibc**, the HBs in **IIb** and **IIIb** should be stronger than that in **Ibc**. But, as can be seen from Table 2, the calculated  $|\Delta E_{SES}|$  are lower for **IIb** and

**Table 2.** B3LYP/6-311G(d,p) Calculated HB properties [R (O...X), and R(O...H) values ( $\text{\AA}$ ), and  $\Delta E_{SE}^s$  (kcal/mol)],  $\rho_b$  ( $e\text{-}\text{\AA}^{-3}$ ) and equilibrium bond lengths,  $R_e$  ( $\text{\AA}$ ) for X–H bonds of all the class I systems investigated<sup>a,b</sup>

	$R_{X-H}$	$\rho_{b,X-H}$	R(O...H)	R (O...X)	Q	$-\Delta E_{SE}$
<b>I</b>	0.998 (0.997)	2.2 (2.2)	1.690 (1.703)	2.582 (2.589)	0.157	13.3 (12.3)
<b>Ia</b>	0.996	2.207	1.679	2.570	0.166	13.4
<b>Ib</b>	1.002	2.166	1.648	2.558	0.146	15.1
<b>Ic</b>	0.999	2.193	1.673	2.568	0.168	14.4
<b>Ibc</b>	1.003 (1.003)	2.159 (2.153)	1.630 (1.634)	2.543 (2.544)	0.156	16.2 (15.4)
<b>IIa</b>	0.991	2.247	1.755	2.628	0.171	10.9
<b>IIb</b>	1.041 (1.040)	1.903 (1.903)	1.507 (1.514)	2.471 (2.474)	0.094	14.5 (13.6)
<b>IIc</b>	0.984 (0.983)	2.301 (2.301)	1.818 (1.839)	2.667 (2.678)	0.197	10.1 (9.2)
<b>IIac</b>	0.981 (0.981)	2.321 (2.321)	1.862 (1.878)	2.695 (2.703)	0.212	8.7 (8.0)
<b>IIbc</b>	0.996	2.193	1.731	2.608	0.162	9.7
<b>IIIa</b>	0.994	2.225	1.713	2.594	0.169	12.1
<b>IIIb</b>	1.031 (1.028)	1.964 (1.977)	1.536 (1.550)	2.488 (2.496)	0.116	13.4 (12.6)
<b>IIIc</b>	0.983 (0.983)	2.315 (2.308)	1.825 (1.830)	2.666 (2.667)	0.192	9.3 (8.8)
<b>IIIac</b>	0.985 (0.985)	2.288(2.281)	1.760 (1.766)	2.607 (2.609)	0.193	10.0 (9.6)
<b>IIIbc</b>	0.994	2.207	1.730	2.606	0.169	8.5
<b>IV</b>	0.984	2.294	1.757	2.635	0.146	10.9
<b>V</b>	0.998	2.193	1.675	2.545	0.171	9.2
<b>VI</b>	1.362 (1.360)	1.451 (1.451)	1.913 (1.933)	3.070 (3.078)		2.4 (2.6)
<b>VII</b>	1.479 (1.478)	1.181 (1.181)	1.972 (2.000)	3.194 (3.203)		-0.9 (-0.8)
<b>VIII</b>	1.021	2.267	2.187	2.972		2.3
<b>IX</b>	1.019	2.281	2.104	2.908		3.7
<b>X</b>	1.020 (1.020)	2.274 (2.274)	2.079 (2.094)	2.871 (2.878)		3.0 (2.9)
<b>XI</b>	1.023	2.261	2.129	2.943		4.2
<b>XII</b>	1.023	2.261	2.137	2.935		3.2

<sup>a</sup> Depending on the system,  $\Delta E_{SE}$  may or may not be equal to  $E_{HB,A}$ .

<sup>b</sup> X = O (for **I**, **Ix**, **Iix**, **IIix**, **IV** and **V**), S (for **VI**), Se (for **VII**), and N (for **VIII–XII**). Values in parentheses are B3LYP/6-311++G(d,p) results.

**IIIb** contradicting the strength predicted by the O...O (and O...H) distances. If the  $\Delta E_{SES}$  of **IIb** and **IIIb** are compared to that of **I** (MAE)—which can be used for calibration purposes—the differences are only of the order of 0.3–1.5 kcal/mol. Accordingly, if the  $\Delta E_{SES}$  were to be interpreted as apparent HB energies, a prima facie inference that suggests the HB strengths among these three systems are similar would be made.<sup>65</sup> Furthermore, juxtaposition of the geometrical<sup>17c,64</sup> and energetic<sup>63</sup> HB strength classification criteria would suggest that **I** should have a strong HB (belonging to the 12–24 kcal/mol classification), while **IIb** and **IIIb** should have nearly very strong HBs (of the order of 24 kcal/mol). Thus, if this rationalization holds, the difference between the  $E_{HB,AS}$  in **I** and **IIb/IIIb** ought to be of the order of 10 kcal/mol, and not a difference of <1.5 kcal/mol (according to the data in Table 2). Even more importantly, the HB stabilization in **I** is about 12 kcal/mol,<sup>59,66</sup> while that in **Ibc** is about 14–15 kcal/mol,<sup>67</sup> that is, in good agreement with that calculated in this work. Hence, the values reported for **I** and **Ibc**, along with the O...O distances in Table 2, may be used for calibration purposes. Accordingly, the HB stabilization in **IIb** and **IIIb** should be significantly greater than that in **Ibc**. Similarly,  $E_{HB,AS}$  of **IIbc**, **IIIbc**, and **V** should be comparable to that of **I** (~12 kcal) as opposed to the values of 8.5–10 kcal/mol given in Table 2.

The above anomalies are not trivial for two reasons: (1) The estimated errors are well outside of the typical experimental error of about 1–2 kcal/mol. (2) If the underestimated values were to be used for correlation purposes, they can be expected to lead, not only to considerable scatter, but also more importantly, they may lead to unphysical and misleading results.<sup>68</sup> One immediate question that arises then is: what is the nature (and the extent thereof) of the perturbation by the substituents that has led to such anomalies? To seek some answers to this question, we have examined the geometries and molecular structures (topological) of a selected set of systems to determine the structural perturbations (by the CH<sub>3</sub>, F, and Cl substituents) that might have led to the intractable interactions (which in turn might have led to the error in the calculated HB SEs).

### Assessment of the causes of the anomalies: cross-correlation analyses

The systems that exhibit significant anomalies in the energetic parameters are **IIb**, **IIIb**, **IIbc**, **IIIbc**, **V**, **VII**, and possibly **VI**. However, the sources of the anomalies are not necessarily the same in every case. This section considers mainly the anomalies in **IIb**, **IIIb**, **IIbc**, and

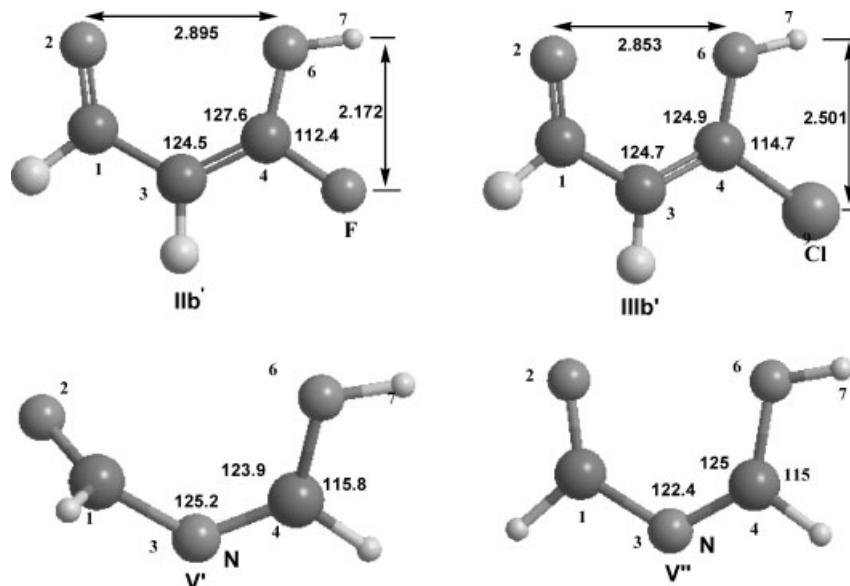


**Figure 1.** Non-H-bonded forms of **IIb**, **IIIb**, and **V**. **IIb'** and **IIIb'** are fully optimized (B3LYP/6-311G(d,p)) non-H-bonded forms of **IIb** and **IIIb** (respectively). **V'** was obtained when the H of the enol of **V** was rotated by 180° and the resulting input geometry was fully optimized (2-1-3-4 dihedral angle = 89°). **V''** was obtained when the same input geometry was constrained to be planar and optimized. The  $\Delta E_{SE}$  value for **V** in Table 2 is the difference between the energies of **V** and **V'**. **V'** is more stable than **V''** by about 3.2 kcal/mol. Distances are in Å and bond angles are in degrees (°)

**IIIbc.** The case of **VII** and **VI** will be addressed in Trend in Energetic ( $E$ ) versus Geometrical ( $G$ ) Consequences Section, and that of **V** both in this section (some details are given in Fig. 1) and in Dissection of  $\Delta E_{SE}$ : Acceptable ( $E_{HSE}$ ) and Non-Acceptable ( $E_{NSE}$ ) Measures of HB Strength section, Trend in Energetic ( $E$ ) Versus Geometrical ( $G$ ) Consequences section, and Natural Bond Orbital Studies section as well.

The anomalies may arise from unequal changes (upon H bonding) in geometry, charge, bond-angle distortion and from differences in the *molecular structures* (i.e., the connectivity schemes governed by the topology of  $\rho$ ).<sup>48,69</sup> To explore such contributions, two types of cross-correlation analyses of the changes in geometry, charge, and bond-angle distortion were made using a selected set of systems, that is, **I**, **Ib**, **IIb**, and **IIIb**: (a) vertical comparison of the various systems with **I**, and (b) horizontal comparison of cC and cO forms of the same molecule. Cross-correlation analyses of the molecular graphs (MGs) of the cC and cO forms (data not shown) were also made. The results of such analyses did not reveal a clear trend. The effects considered did not also appear to be significant enough to contribute to the observed anomalies in the energetic parameters. Hence, the details are not provided here, but are given as Supplementary Material. On the other hand, H...F/Cl interactions (and O...F/Cl interactions to a marginal degree), which are found to make significant contributions, are discussed briefly below.

**Horizontal cross-correlation analyses of H...F/Cl and O...F/Cl interactions.** In the cO forms of the  $\beta$ -halo derivatives (but not in the cC forms), intramolecular H...F and H...Cl interactions are possible between the H of the enol and the F/Cl atoms (Fig. 1). The H...F and H...Cl distances (Fig. 1) are 2.172 and 2.501 Å in, respectively, **IIb** and **IIIb**, that is, well below the corresponding sums of the Pauling's van der Waals radii (2.55 and 3.01 Å).<sup>70a</sup> Very preliminary estimates indicate the contribution of these interactions [primarily due to van der Waals forces in accordance with our AIM analysis<sup>48,70c</sup>] to the stabilization in the cO forms of **IIb** and **IIIb** may be of the order of 3 kcal/mol. This would reduce the respective  $\Delta E_{SES}$  (in absolute terms), and hence would lead to the underestimation of  $E_{HB,A}$ . Because of the  $\beta$ -halo substitutions in **IIbc** and **IIIbc** (as in **IIb** and **IIIb**), the same type of interactions will also lead to the underestimation of  $E_{HB,A}$  in **IIbc** and **IIIbc** as well. These kinds of interactions have been observed recently in similar cases.<sup>53c</sup>

**O...F/Cl Interactions.** Our analysis does not suggest repulsions between the lone pairs of the O6 and F/Cl atoms would lead to greater O...O contractions. However, O...F and O...Cl interactions may impact the relative SEs in another way. Upon hydrogen bonding, the C—F, C—Cl, and C4—O6 bond lengths decrease (Supplemental Material, Figure S1) without a significant widening of angles F—C4—O6 and Cl—C4—O6 (Supplemental Material, Figure S2). This effect, in turn, decreases the



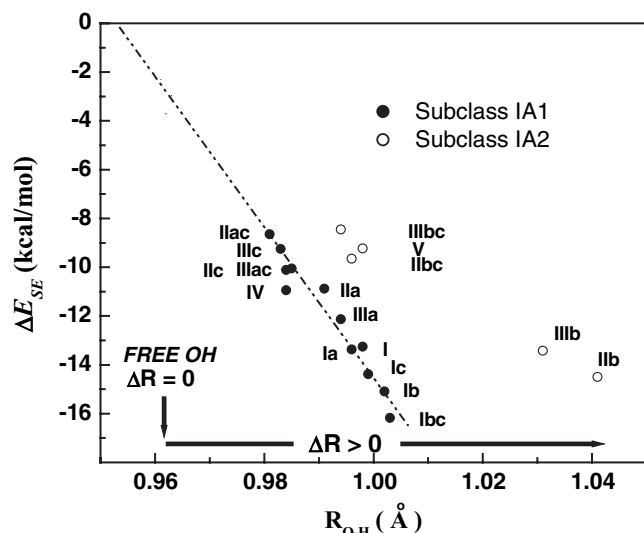


**Figure 3.** Plot of  $\Delta E_{SE}$  against the O–H bond distance, and the dissection of the  $\Delta E_{SE}$  values into acceptable ( $E_{HSE}$ ) and non-acceptable ( $E_{NSE}$ ) measures of HB strength. The region of elongation of the O–H bond ( $\Delta R > 0$ ) has been indicated roughly. The unfilled circle data points (subset IA2 whose  $\Delta E_{SE} = E_{NSE}$ ) show deviation from the trend observed (dotted line) for the filled circle data points (subset IA1 whose  $\Delta E_{SE} = E_{HSE}$ ). This Figure is to be compared to Fig. 2

filled-circle data points. We will identify the latter set of 12 systems (**I**, **Ia**, **Ib**, **Ibc**, **Ic**, **IIa**, **IIac**, **IIc**, **IIIa**, **IIIac**, **IV**, and **IIIc**) as subclass IA1 hereafter. The observed trend is consistent with the observation of Palomar *et al.*<sup>62a</sup> who found a linear correlation between O–H bond lengths and IMHB energy. This analysis, therefore, confirms the  $\Delta E_{SES}$  of systems **IIb**, **IIIb**, **IIbc**, **IIIbc**, and **V** are not acceptable measures of the HB strength. This set of systems will be identified hereafter as subclass IA2.

The case of **IIb**, **IIIb**, **IIbc**, and **IIIbc** has already been rationalized (*vide supra*, Assessment of the Causes of the Anomalies: Cross-Correlation Analyses section). In the case of **V**, the deviation from the general trend can be ascribed to: (a) the optimized cO form not being planar; this diminishes the magnitude of  $\Delta E_{SE}$  by about 3 kcal/mol according to our preliminary estimates (see Fig. 1 for details), (b) the shorter C=N and C–N bonds, compared to the C=C and C–C bonds, and the smaller N atom (relative to C) bringing the O atoms closer without necessarily strengthening the HB (this point will be confirmed later), and (c) the greater N ↔ O6 lone pair–lone pair repulsive interaction in the cC form vis-à-vis that in the nonplanar cO form.

**Further verification on the basis of complementary results.** Although the  $R(G)$  and  $R(\rho_b)$  rankings are in good agreement with each other when it comes to identifying the strongest and weakest H-bonded systems (with O···H—O HB motifs), some discrepancies are also evident when it comes to systems in between the two regimes. This may be because the different parameters may not reflect the culmination of the various subtle modulations<sup>81</sup> (which affect the H bonding) to the same degree. Thus, consideration of various other measures of HB strength is essential. Table 3 compiles such data.<sup>82</sup> For comparison purposes, also included in Table 3 are the types of data presented so far. The data in Table 3 show excellent qualitative internal consistency with the exception of the  $\Delta E_{SE}$  data. Nonetheless, the different parameters do not still give exactly the same quantitative trend,<sup>83</sup> because no two parameters can effectively reflect all the nuances of the interactions which arise from the interplay of various subtle modulations.<sup>81</sup> In any case, the trend obtainable on the basis of the  $V_b$  and  $H_b$  parameters (Table 3) is:

**Table 3.** Comparison of various measures of the strengths of intramolecular hydrogen bonds determined at the B3LYP/6-311G(d,p) level<sup>a</sup>

Parameter	<b>I</b>	<b>Ib</b>	<b>Ibc</b>	<b>IIb</b>	<b>IIIb</b>	<b>V</b>	<b>Ia</b>	<b>IIbc</b>	<b>IIIbc</b>	<b>IIa</b>	<b>IV</b>
$-\Delta E_{SE}$	13.3	15.1	16.2	14.5	13.4	9.2	13.4	9.7	8.5	10.9	10.9
$R(O\cdots O)$ (Å)	2.589	2.559	2.543	2.474	2.496	2.545	2.57	2.608	2.606	2.628	2.635
Q parameter	0.157	0.146	0.156	0.094	0.116	0.171	0.166	0.162	0.169	0.171	0.146
$\rho_b(O\cdots H)$ (e. Å <sup>-3</sup> )	2.2	2.166	2.159	1.903	1.964	2.193	2.207	2.193	2.207	2.247	2.294
$\Delta R$ (Å) <sup>b</sup>	0.036	0.039	0.04	0.075	0.066	0.034	0.034	0.029	0.029	0.029	0.029
$10^{-2}\Delta\nu$ (cm <sup>-1</sup> )	6.546	7.302	7.532	13.012	11.897	6.235	6.424	5.568	5.514	5.448	4.034
$R(O\cdots H)$ (Å)	1.703	1.651	1.63	1.514	1.550	1.675	1.679	1.731	1.730	1.755	1.757
$\rho_b(O\cdots H)$ (e. Å <sup>-3</sup> )	0.337	0.378	0.391	0.54	0.499	0.351	0.344	0.304	0.304	0.290	0.283
$-H_b$	4.4	6.1	6.9	16.2	13.5	4.9	4.7	2.8	2.7	2.3	1.9
$-V_b$	30.4	34.8	36.9	54.6	49.7	32.4	31.5	25.7	25.8	24.5	24.2
$-V_b^c$	28.86	34.23	36.38	53.07	47.36	30.98	31.01	23.58	25.5	23.92	
$-E_{HB,E}^d$	13.3	14.7	15.6	21.1	19.6	15.5	14	12	12.1	11	10.7

<sup>a</sup> Units for  $V_b$  and  $H_b$  are in kcal/mol per atomic unit volume (a.u.v.), and for  $\Delta E_{SE}$ ,  $E_{HB,E}$  and  $E(2)$  in kcal/mol.

<sup>b</sup>  $\Delta R$  is the elongation of the O–H bond.

<sup>c</sup> Data are determined at the B3LYP/6-311++G(d,p) level.

<sup>d</sup>  $E_{HB,E}$ s are estimated in an empirical manner using  $E_{HSE}-R(O\cdots O)$  regression function discussed in Trend in Energetic ( $E$ ) Versus Geometrical ( $G$ ) Consequences section.

- $V_b(H_b)$ : **IIb** > **IIIb** >> **Ibc** > **Ib** > **V** > **Ia** > **I** > **IIIbc** > **IIbc** > **IIa** > **IV**

This trend verifies how the HB strengths of the systems of subclass IA2 should mesh with those in subclass IA1. The data in Table 3 can also be used to quantify the relative HB strengths using a suitable reference such as **I** or **Ibc**. The data also show the  $R(\rho_b)$  ranking is more in line with the above ranking while the O...O distance trend is not quite so.

One of the main points of the preceding discussion is this simple one: information on the electronic bases of the H bonding (as determined here by the AIM formalism) is essential for the verification of the predictions of HB strengths on the basis of energetic and geometrical consequences, and for a more quantitative assessment of the relative strengths of the HB interactions. More will also be said in Nature of the IMHB Interactions and Energy Density- $R(O\cdots H)$  Correlation section regarding other uses provided by the  $V_b$  and  $H_b$  parameters.

## COMPARISON OF NAPHTHAZARIN (NZ) WITH SUBCLASS IA SYSTEMS

As alluded to earlier, for the sake of brevity, consideration of all the class II systems is not feasible in this communication. Accordingly, the discussion in this section will focus on NZ (Chart 1) only. The nature of the structural perturbations in NZ (in system **IV** as well) and subclass IA systems might be expected to be different—owing to the different resonant spacers connecting the HB donor–acceptor segments (see Charts 1 and 3).<sup>56,84</sup>

Insight into the HB interactions in NZ and the subclass IA systems can be gleaned using parameters at the HBCPs (BCPs at the O...H HB). Selected topological properties, including potential ( $V(r)$ ) and total ( $H(r)$ ) energy densities,<sup>20</sup> at the HBCPs (denoted by subscript b) are given in Table 4. These parameters can be used for cross-comparison of the cC forms. The  $H_b$  values are negative (indicating the interactions are stabilizing). The values of both  $V_b$  and  $H_b$  follow the decreasing suborder **IIb** > **IIIb** > **Ibc** > **Ib** > **I** > **NZ**. This finding strongly supports the  $R(G)$  ranking provided previously in Prefatory Calibration of the Energetic and Geometrical Parameters section. Similarly, the values of  $\rho_b$  also lead to the same trend. By contrast, no clearly discernable trend can be obtained from the  $\nabla^2\rho_b$  data. In fact, the values for NZ are roughly 8–9 times more than those shown for the systems in Table 4. Whether this result is a manifestation of the fused aromatic ring needs further investigation.

Figure 4 shows a plot of  $E_{HSE}$  and  $E_{NSE}$  versus  $V_b$ . Included in Fig. 4 are also data for NMA [a very strong IMHB system, Chart 3]<sup>64</sup> and for BAA (a low barrier HB (LBHB) system, Chart 3),<sup>41</sup> the  $\Delta E_{SE}$  values of which were taken from the literature.<sup>41,64</sup> The plot shows, NZ as

**Table 4.** B3LYP/6-311G(d,p) calculated O...O and O...H distances, and selected topological properties of  $\rho$  at the (3,−1) hydrogen bond critical points (b)<sup>a</sup>

S <sup>b</sup>	R(O...O)	R(O...H)	$\rho_b$	$\nabla^2\rho_b$	$-V_b$	$-H_b$
<b>I</b>	2.582	1.69	0.3387	3.31	30.3	4.4
<b>Ib</b>	2.558	1.648	0.3759	3.479	34.9	6.14
<b>Ibc</b>	2.543	1.63	0.3916	3.562	36.9	6.9
<b>IIb</b>	2.471	1.507	0.5582	3.377	57.1	17.6
<b>IIIb</b>	2.488	1.536	0.4959	3.508	49.4	13.3
<b>NZ(A)</b>	2.5880	1.7022	0.3257	3.388	29.15	3.55
<b>(B)</b>	2.5887	1.7026	0.3253	3.391	29.1	3.54

<sup>a</sup> Units for R(O...O) and R(O...H) are Å; for  $\rho_b$ : e.Å<sup>−3</sup>; for  $\nabla^2\rho_b$ : e.Å<sup>−5</sup>; for energy densities ( $V_b$  and  $H_b$ ): kcal/mol per atomic unit volume (a.u.v.).

<sup>b</sup> Molecular system; (A) and (B) denotes the two H-bonded segments of NZ.

well as NMA<sup>64</sup> and BAA<sup>41</sup> conform to the general trend observed. Thus, the very different nature of the resonant spacer in NZ did not lead to a deviation from the trend for subclass IA1. To gauge the strength of the IMHB in NZ relative to that of **I** and **Ibc** (as well as to that of NMA and BAA), the  $V_b$ -based decreasing suborder in HB strength can be considered: **NMA** >> **IIb** > **IIIb** > **BAA** > **Ibc** > **Ib** > **I** > **NZ**.

Finally, there is one particularly noteworthy conclusion from this section. Despite the very different nature of the resonant spacers connecting the HB D-A segments, the data in Table 4 and the plot in Fig. 4 (and Fig. 5, vide infra) provide with conclusive evidence that the IMHB strength in NZ is comparable to that of MAE (**I**).

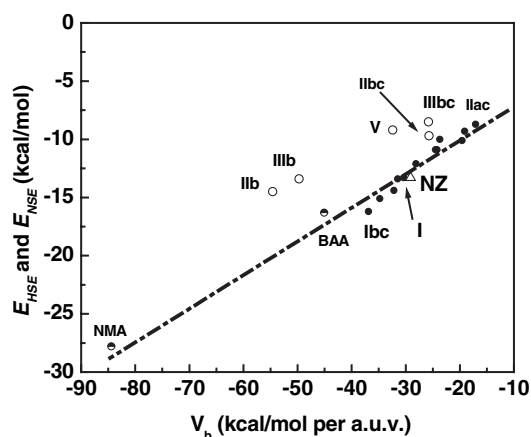


**Figure 4.** Scatter plot of  $E_{HSE}$  and  $E_{NSE}$  vs.  $V_b$  showing the deviation of the  $E_{NSE}$  values from the trend line. Only O–H...O systems are included. Filled circles are  $E_{HSE}$ s of subclass IA1; unfilled circles are  $E_{NSE}$ s of subclass IA2; the unfilled triangle is for  $E_{HSE}$  of NZ; half-filled circles are for nitromalonamide (NMA) and benzoylacetone (BAA) whose apparent HB energies were taken from references 64 and 41, respectively

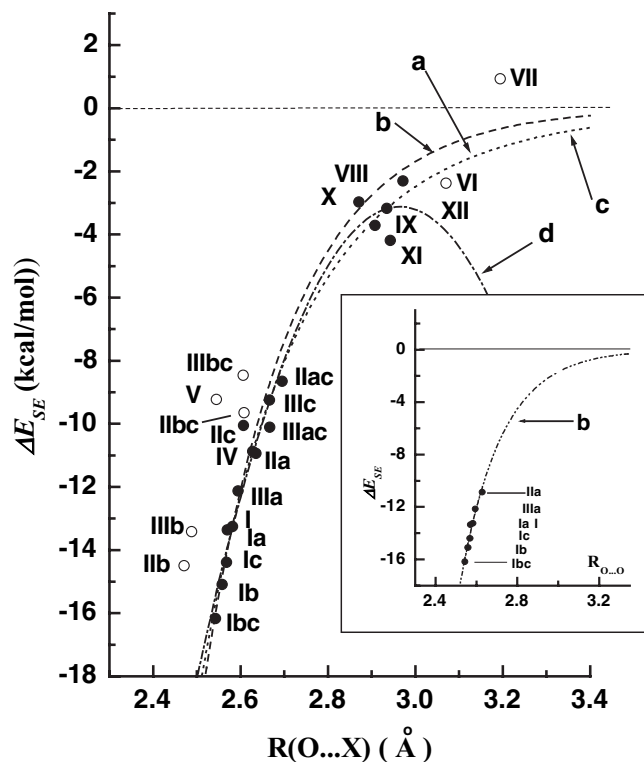


**Figure 5.** A scatter plot of  $\Delta E_{SE}$  (kcal/mol) versus  $R(O\cdots X)$  ( $X=O, N$ ) distance. Subclass IA2 and IB1 systems (unfilled-circle data points with  $E_{NSE}$  values) were included for completion purposes only, and were not used in the regression analyses. For curves **a**, **c**, and **d**, subclasses IA1 and IB2 (filled-circle data points) were used. Curve **b** of the inset Figure was independently obtained using a subset of subclass IA1 (systems with  $R(O\cdots O) \leq 2.65$  Å as labeled in the inset Figure). The regression function for this curve was later added to the main Figure to demonstrate the behavior of curves **a**, **c**, and **d** is not merely the influence of the data for the subclass IB2 systems. The regression functions (for data points with filled circles only) are, for curve **a** (exponential): Eqn (2) (given in the text); curve **b** (exponential; inset):  $E_{HSE} = -4.364 \times 10^6 \exp(-4.92 R(O\cdots O))$  ( $R^2 = 0.960$ ); curve **c** (inverse-power law):  $\Delta E_{SE} = (5.109 \times 10^5 R(O\cdots X))^{-11.14}$  ( $R^2 = 0.977$ ); curve **d** (parabolic):  $\Delta E_{SE} = -69.3 R(O\cdots X)^2 + 410.87 R(O\cdots X) - 612.14$  ( $R^2 = 0.974$ ). For curves **a**, **c**, and **d**,  $\Delta E_{SE} = E_{HSE}$  for subclass IA1 systems.

## TREND IN ENERGETIC (E) VERSUS GEOMETRICAL (G) CONSEQUENCES

### $E_{HSE}-R(O\cdots X)$ correlation

Figure 5 shows a scatter plot of  $\Delta E_{SE}$  versus  $R(O\cdots X)$  [ $O\cdots X$  distances] which includes data for systems in four subclasses. Subclass IA1 (for which  $\Delta E_{SE} = E_{HSE}$ ) and subclass IB2 are represented by filled-circle data points. Subclasses IA2 and IB1 are represented by unfilled circles. Subclass IA2 systems (**IIb**, **IIbc**, **IIIb**, **IIIbc**, and **V**) should be excluded from the  $E \leftrightarrow G$  regression analysis because their  $\Delta E_{SE}$ s are not acceptable indicators of their IMHB strengths. The subclass IB1 systems (**VI** and **VII**,

cf. Chart 3) should also be excluded from the analysis for the following reason. The open (cO) form of **VII** is found to be more stable as reflected by the positive value of  $\Delta E_{SE}$  (Table 2). What makes the cO form of **VII** more stable can be attributed to the attractive  $O\cdots Se$  interaction, as reported before.<sup>85</sup> The positive (destabilizing)  $\Delta E_{SE}$  value cannot therefore represent the HB strength in **VII**. In like manner, the  $\Delta E_{SE}$  of **VI** is likely to be influenced by the  $O\cdots S$  attractive forces in the cO form.<sup>85c-d</sup> NZ is not also included, but instead is used as a test case to show the regression function for the  $E \leftrightarrow G$  correlation can predict its apparent HB energy ( $E_{HB,A}$ ).

Accordingly, the curve fitting analyses were done using the subclasses IA1 and IB2 systems only (i.e., data points with filled circles consisting of  $O\cdots H-O$  and  $O\cdots H-N$  HB motifs; or,  $X=O, N$  cases). Very similar results are obtained when  $R(O\cdots H)$  is used instead (plot not shown). Three different models were attempted. The curves obtained (see Fig. 5 for details) are labeled **a** (exponential), **c** (inverse-power), and **d** (parabolic/quadratic).<sup>86</sup>

**Consistency and asymptotic behavior.** Two important conclusions concerning the fundamental behavior of the  $E \leftrightarrow G$  correlation in Fig. 5 can be noted. (1) The behavior (including the asymptotic feature) manifested by curves **a**, **b**, and **c**, and hence by the  $E_{HSE}-R(O\cdots X)$  ( $X=O, N$ ) correlation, is consistent with the standard behavior manifested by intermolecular HBs.<sup>2,20</sup> (2) By contrast, curve **d**—the concave downward parabolic curve—although it has a high degree of fidelity, is obviously unphysical at large distances, that is, it does not conform to the asymptotic phenomenological behavior of HB interaction energies at large distances.<sup>2,20</sup> Hence, this quadratic model has to be rejected despite the good correlation obtained for it. An important point worthy of note here: the behavior demonstrated by curves **a**, **b** (see Fig. 5 for details), and **c** is at variance with the quadratic (concave upward) behavior reported in Refs. 23 and 24.<sup>87</sup>

**Predictive ability of the  $E_{HSE}-R(O\cdots O)$  parametric model.** An important utility of the  $E_{HSE}-R(O\cdots O)$  regression function would be its use as a predictive model for the estimation of apparent HB energies in an empirical manner—identified by  $E_{HB,ES}$  hereafter. Accordingly, several sample calculations of  $E_{HB,ES}$  were made using (Eqn (2)).

$$E_{HSE} = -5.554 \times 10^5 \exp(-4.12 R(O\cdots X)) \quad (2)$$

$$(X = O, N; \Delta E_{SE} = E_{HSE} \text{ for subclass IA1}) [n = 17 \text{ (data points)}; R^2 = 0.975]$$

In particular,  $E_{HB,ES}$  of  $-21$  and  $-19.1$  kcal/mol were calculated, respectively, for **IIb** and **IIIb** as opposed to  $\Delta E_{SE}$ s of, respectively,  $-13.6$  and  $-12.6$  kcal/mol given in Table 2. This indicates the apparent HB energies of **IIb**

and **IIIb** were grossly underestimated by as much as 7–8 kcal/mol. Consequently, this finding confirms that the HB interactions in **IIb** and **IIIb**, when compared to **I**, should be about 1.5–1.6 times as strong—in line with the AIM and NBO results (presented herein). Similarly,  $E_{\text{HB,ES}}$  have been calculated for NMA,<sup>64</sup> BAA,<sup>41</sup> NZ, and for MAE and other derivatives reported in Ref. 53. In all cases, the  $E_{\text{HB,ES}}$  thus estimated were in excellent agreement (within the limits of <2 kcal/mol of experimental error) with those reported,<sup>88</sup> convincingly demonstrating the exponential parametric model has predictive ability.

The  $E_{\text{HB,E}}$  estimate for NZ (–13 kcal/mol) when compared with the  $\Delta E_{\text{SE}}$  estimated by Eqn (1) (–13 kcal/mol as reported before by us<sup>14</sup>) indicates Eqn (2) can successfully reproduce the  $\Delta E_{\text{SE}}$  ( $=E_{\text{HSE}}$ ) value for NZ. It will also be shown in a future communication that Eqn (2) can successfully estimate  $E_{\text{HB,AS}}$  for other class II systems as well. *This is a noteworthy finding. Because, despite the very different nature of the resonant spacers connecting the HB D-A segments, the two classes of systems (including NMA and BAA) are governed by the same  $E \leftrightarrow G$  correlation.*

**Verifiability of the  $E \leftrightarrow G$  correlation.** To independently confirm the validity of the  $E \leftrightarrow G$  correlation of Fig. 5, the correlation that would obtain between  $E_{\text{HB,E}}$  (computed via Eqn (2)) and the energy density parameters at the HBCP,  $H_b$  and  $V_b$  [ $V_b$  has been shown in the intermolecular case to be approximately proportional to the HB interaction energy<sup>20,89</sup>] has been sought. Figure 6

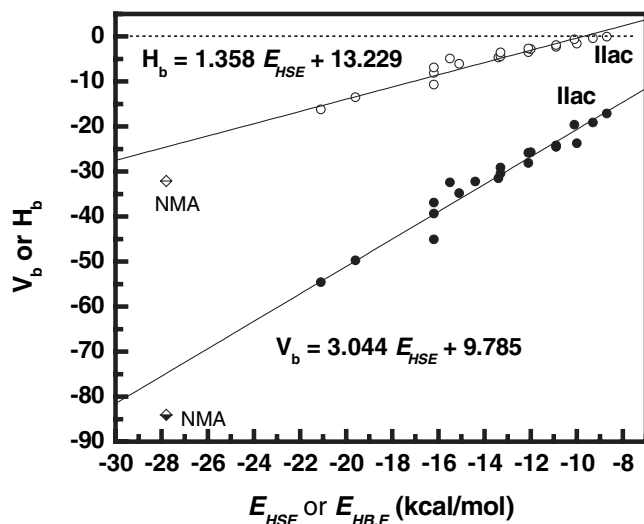


**Figure 6.** Graphical illustration of the predictive ability of the  $E_{\text{HSE}}\text{-R}(\text{O}\cdots\text{O})$  parametric model (Eqn (2)). Only O–H $\cdots$ O systems are included. This Figure is to be compared with Fig. 4. The plots show the correlation of both  $V_b$  and  $H_b$  (both in kcal/mol per atomic unit volume) with the apparent HB energies  $E_{\text{HSE}}$  and  $E_{\text{HB,E}}$ . For this plot, corresponding  $E_{\text{HB,E}}$  values have been used in place of  $E_{\text{NSE}}$ s of subclass IA2. The plot shows noticeable deviation in the case of NMA, and the factor responsible has not been fully investigated yet

shows such plots of  $V_b$  and  $H_b$  versus  $E_{\text{HSE}}$  or  $E_{\text{HB,E}}$ . That is, the  $E_{\text{NSE}}$  values in Fig. 4 have been replaced by  $E_{\text{HB,ES}}$ . The correlation obtained has a high degree of fidelity<sup>90</sup> in both cases, with the regression functions found being

$$V_b = 3.044 E_{\text{HB}} + 9.785$$

$$\{R = 0.985; n = 22 \text{ data points}; S_D = 2.17\}$$
(3)

$$H_b = 1.358 E_{\text{HB}} + 13.229$$

$$\{R = 0.976; n = 21 \text{ (data points)}; S_D = 1.24\}$$
(4)

wherein  $E_{\text{HB}}$  represents  $E_{\text{HSE}}$  and/or  $E_{\text{HB,E}}$ . Therefore, the correlated behavior strongly confirms the validity, and soundness, of the exponential  $E_{\text{HSE}}\text{-R}(\text{O}\cdots\text{O})$  relation (Eqn (2)).

The correlations obtained above can be used to demonstrate the advantage of the combined use of QC and AIM calculations. The  $E_{\text{HB,E}}$  predicted for system **V** by Eqn (2) is –15.5 kcal/mol (Table 3). If, as pointed out in Dissection of  $\Delta E_{\text{SE}}$ : Acceptable ( $E_{\text{HSE}}$ ) and Non-acceptable ( $E_{\text{NSE}}$ ) Measures of HB Strength section, the R(O $\cdots$ O) distance for **V** is forced to be too short, the  $E_{\text{HB,E}}$  predicted by Eqn (2) would then be too large. On the other hand, if one uses Eqn (3) and Eqn (4) to estimate  $E_{\text{HB,E}}$ , an average value of –13.6 kcal/mol that is comparable to that of **I** is calculated. This confirms that the HB strength of **V** and **I** should be comparable. Hence, whereas the geometrical consequence (O $\cdots$ O distance) is not a good indicator of the HB strength in the case of **V**, the energy densities allow better estimates for the energies of the HB formation.

**$E_{\text{HSE}}\text{-R}(\text{O}\cdots\text{O})$  correlation based on MP2 results.** To make the  $E_{\text{HB,ES}}$  more in line with the MP2/6-311++G(d,p) results, the MP2 data in Table 1 were plotted (as shown in Fig. 7) to obtain the regression function sought. The regression function obtained for the filled circle data points was (Eqn 5):

$$E_{\text{HSE}} = -8.426 \times 10^5 \exp(-4.333 R(\text{O}\cdots\text{O}))$$

$$\{R^2 = 0.919; n = 9 \text{ (data points)}\}$$
(5)

The fitting was done by excluding the data for **IIb** and **IIIb** (as in Fig. 5).

Overall, the results of the analyses made indicate both  $E_{\text{HSE}}$  and  $E_{\text{HB,E}}$  are acceptable measures of the IMHBs. The relative strengths as determined from AIM (as well as from NBO) parameters should, however, be accurate because they are determined independent of the non-H-bonded forms. Nevertheless, the availability of more accurate approaches is always desirable. In this connection, one of the few approaches<sup>89,91</sup> that have been proposed for the calculation of the SEs of IMHBs is the use of a modified Grabowski complex parameter,<sup>24</sup> advanced by Chen and Naidoo.<sup>92</sup> This approach has been shown to be very suitable especially for molecules with

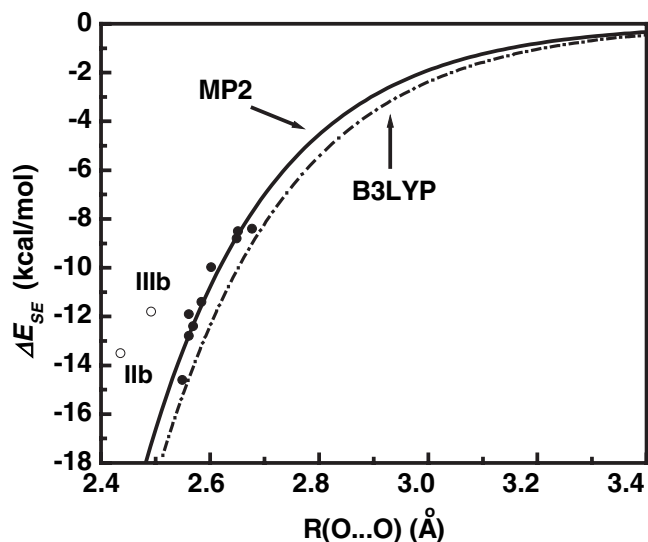


**Figure 7.** A plot of MP2-calculated  $\Delta E_{SE}$  (kcal/mol) versus  $R(O\cdots O)$  distance. The unfilled circle data points were not included in the curve fitting. The Figure also compares the MP2/6-311++G(d,p) curve with that of the B3LYP/6-311G(d,p) curve (Eqn (2)). Except for some quantitative differences, the two curves are in very close agreement.

multiple HBs found in close proximity to each other.<sup>91</sup> The use of this approach for the study of very strong IMHBs<sup>93</sup> may thus be explored in future work. On the other hand, we should note here that we have analyzed the correlation of the predicted  $E_{HB,E}$  values with the electron density  $\rho_b$  at the O-H BCP and with the differential in  $\rho_b$  upon H bonding (data not shown). The good linear correlations found (with  $R=0.972$  and  $R=0.985$ , respectively) are implicitly consistent with the Chen and Naidoo results,<sup>92</sup> as well as with the recently reported linear correlation of intermolecular HB energy with  $\rho_b$  at the HB BCP.<sup>94</sup>

## NATURE OF THE IMHB INTERACTIONS AND ENERGY DENSITY- $R(O\cdots H)$ CORRELATION

The exponential  $E_{HSE}-R(O\cdots O)$  regression function (Eqn (2)) cannot be used to estimate the  $E_{HSE}$  of systems like **VI** and **VII**. However, the IMHB strengths of all the homo- and heteronuclear HBs can be assessed within the tenets of the AIM theory. Accordingly, 'closed-shell' and 'shared' interaction limits can be considered using the following two fundamental relations (Eqn (6) and Eqn (7)):<sup>29,95</sup>

$$(\hbar^2/4m)\nabla^2\rho(r) = 2G(r) + V(r) \quad (6)$$

$$H(r) = V(r) + G(r) \quad (7)$$

where  $\nabla^2\rho(r)$  is the Laplacian of the charge density,  $G(r)$  the electronic kinetic energy density and  $V(r)$ <sup>29</sup> the electronic potential energy density. [Usually the corresponding BCP parameters are denoted by  $\nabla^2\rho_b$ ,  $G_b$

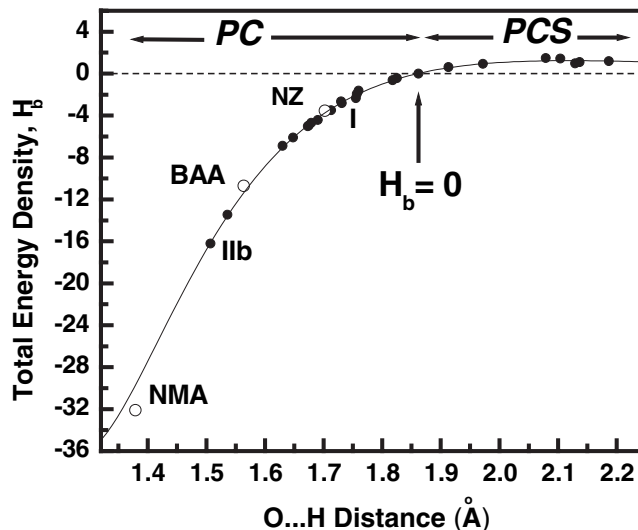


**Figure 8.** A plot of  $H_b$  (kcal/mol per a.u.v) vs. HB distance,  $R(O\cdots H)$  for all systems. PC and PCS denote respectively, partially covalent and purely closed-shell. The solid curve is the regression fitting line obtained using the data (filled circles) for all class I systems (Chart 2). Unfilled-circle data points (not included in the regression analysis) are for NZ, NMA, and BAA. The actual regression function obtained was (24 data points;  $R^2=0.999$ ):  $1.789 \times 10^3 R(O\cdots H)^{-8.08} - 2.9656 \times 10^5 \exp(-5.443 R(O\cdots H))$ . The dependence of  $H_b$  on  $R(O\cdots O)$  (plot not shown) also gave very similar results

(always positive),  $V_b$  (always negative), and  $H_b$  (may be positive or negative depending on the values of  $G_b$  and  $V_b$ ). In this context, shared interactions are dominated by lowering the potential energy  $V(r)$ , and are obtained when  $\nabla^2\rho_b < 0$  [or when  $|V_b| > 2G_b$ ]. By contrast, 'purely closed-shell' interactions are obtained when both  $H_b > 0$  and  $\nabla^2\rho_b > 0$ . The intermediate region between these two limits, that is, interactions with  $H_b < 0$  and  $\nabla^2\rho_b > 0$ , may be characterized as *partially covalent*.<sup>96-98</sup> Also, the magnitudes of  $V_b$  and  $H_b$  represent the capacity of the system to concentrate electrons at the HBCP.<sup>20</sup> Consequently,  $V_b$  and  $H_b$  should be very useful for a comparative study of the strengths of IMHBs with different HB motifs as is the case in this study.<sup>20</sup> We focus here on the behavior of only  $H_b$ , because the  $H_b$  parameter is more suitable to determine the nature of the interactions.

Figure 8 shows the dependence of  $H_b$  on  $R(O\cdots H)$  of the X—H $\cdots$ O bridge (X=O, N, S, Se). The data were fitted with a sum of power law and exponential functions:  $P_1d^{-P_2} + P_3 \exp(-P_4d)$  where  $d=R(O\cdots H)$ , using four unweighted parameters ( $P_1$ ,  $P_2$ ,  $P_3$ , and  $P_4$ ). The plot shows that there is a negative-to-positive cross over at about  $R(O\cdots H) \sim 1.86$  Å where  $G_b \sim |V_b|$  and  $H_b = 0$ . The near equality also means that  $(\hbar^2/4m)\nabla^2\rho_b \sim G_b$  in accordance with Eqn (6). At values of  $R(O\cdots H) < 1.86$  Å,  $G_b < |V_b|$ , and  $H_b < 0$ . The  $H_b < 0$  cases indicate the accumulation of charge in the internuclear region is stabilizing, indicating the respective IMHBs have varying degrees of partial covalency.<sup>96-98,62g</sup> The subclass IA systems (Table 2), BAA, NMA, and NZ (including all of

the other class II systems, data not shown) meet this criterion. Hence, the interactions are *partially covalent*. Also, because  $H_b < 0$  for these systems,  $|V_b| > G_b$ , and the charge accumulation is net stabilizing. In fact, out of all the systems in Table 2,  $\rho_b$ ,  $V_b$ , and  $H_b$  are the highest and the second highest, respectively for **IIb** and **IIIb**—the ratios being roughly 1.6–1.8 times relative to that of **I**.

At values of  $R(O\cdots H) > 1.86 \text{ \AA}$ ,  $G_b > |V_b|$ , and  $H_b > 0$ , and the interaction is destabilizing. This region is the 'purely closed-shell' region.<sup>96–98,62g</sup> In our case, the IMHBs represented in this region are heteronuclear HBs, which are expected to show hindered covalency partly because the X—H bond in X—H $\cdots$ Y is stretched only slightly,<sup>56b</sup> or may even contract as is observed for improper HBs.<sup>73</sup>

## NATURAL BOND ORBITAL STUDIES

In this section, we consider the electronic bases of the H bonding from the perspectives of the NBO theory.<sup>30</sup> The NBO approach can be expected to provide with several advantages/facilities<sup>30,99–104</sup> (See Ref. 99 for details). However, the rationale for our use of the NBO approach is predicated by this main attribute of the method: charge transfer (CT) from lone pair and/or bonding orbitals of the HB acceptor to the antibonding orbitals of the HB donor has been found to be fundamental in HB interactions.<sup>30,102</sup> Hence, the focus in this report is mainly on the qualitative and 'quantitative' predictions of the strength of the H bonding that can be made on the basis of the perturbative HB donor–acceptor interaction energies. It should, however, be noted that our use of the word 'quantitative' here and in the rest of the report is to be understood for the most part in a relative sense.<sup>105</sup> We will also seek to get insight into the effects of substituents on the HB strengths. Such considerations can be extremely useful especially in those cases where intractable interactions may be involved, as is the case in this study.

The NBO discussion that follows will be concerned only with those systems in Subclass IA (all possessing —O—H $\cdots$ O=C— IMHB motifs) with the exception of system **IV**. Essentially all of the systems in Subclass IA are highly delocalized systems. Hence, a multitude of donor  $\rightarrow$  acceptor (D-A) stereoelectronic interactions (SIs) obtain. Due to this reason, a report on a detailed analysis of all the SIs of all the systems is not feasible in this communication (in terms of space). Instead, the discussion will focus only on the HB D-A hyperconjugative (HC) SIs. A cross correlation analysis using a selected set of systems will also be made using **I** (which has been extensively investigated, and is well understood,<sup>15–17</sup>) as a check to gauge the strengths and weaknesses of a given technique. Hence, the cross correlation analysis has been done relative to the data for **I**. We should note here that the NBO theory has been used before for similar purposes.<sup>100,106–109</sup>

## HB D-A hyperconjugative stereoelectronic interactions (HCSI<sub>hb</sub>)

The NBO results show CT occurs from several donor orbitals to the acceptor O6–H7 antibond ( $\sigma^*(O—H)$ ). However, the primary donor orbital for the CT to the  $\sigma^*(O—H)$ , in the cC forms, is the  $n_\sigma(2)O2$  orbital, followed by  $n_\sigma(1)O2$ , that is, the two donor orbitals of the HCSI<sub>hb</sub>s (Chart 4). By contrast, the only HCSI involving the  $\sigma^*(O—H)$  in the cO forms is the  $\sigma(C3—C4) \rightarrow \sigma^*(O—H)$  interaction. The second-order interaction energy  $E(2)$  for this SI is less than half that of the  $n_\sigma(1)O2 \rightarrow \sigma^*(O—H)$  interaction in the cC forms. To illustrate the dominant nature of the CT from the  $n_\sigma(2)O2$  orbital, relevant parameters are provided in Table 5 for the selected set of systems—namely, the  $\beta$ -CH<sub>3</sub> (**Ib**), -fluoro (**IIb**), and -chloro (**IIIb**) derivatives of **I**.

Comparison of the data in Table 5 shows the F and Cl  $\beta$ -substitutions increase the  $E(2)$  of the  $n_\sigma(2)O2 \rightarrow \sigma^*(O—H)$  interaction dramatically (by 232 and 172%, respectively). That is, the D-A ability of this SI is enhanced dramatically by the  $\beta$ -halo substitution. By contrast, the enhancement by the CH<sub>3</sub>  $\beta$ -substitution is much less. Accordingly, the occupancies of the  $\sigma^*(O—H)$  NBOs, which are less than 10 me in the cO forms, increase to about 63–116 me upon H bonding with the net CT being, respectively: 0.10801 e (**IIb**) > 0.09469 e (**IIIb**) > 0.0641 e (**Ib**) > 0.05739 e (**I**). Most importantly, the HCSI<sub>hb</sub> D-A ability that follows the order **IIb** > **IIIb** > **Ib** > **I** is found to be consistent with the order obtainable on the basis of O $\cdots$ O distances [ $R(O\cdots O)$ ], and not with the binding energy (for H bonding) estimates derived through the use of Eqn (1). This provides strong evidence that  $R(O\cdots O)$  is a reasonable indicator of the relative strength of the IMHBs. These results and observations are also consistent with the AIM results presented in earlier sections.

**NBO charge transfer vis-à-vis energy of HB formation.** It has been established that CT, as reflected by the second-order interaction energy,  $E(2)$ , results in an increase in binding energy.<sup>30</sup> As noted above, the D-A ability of the HB interaction is dominated by the  $n_\sigma(2)O2 \rightarrow \sigma^*(O—H)$  interaction (with its SI energy

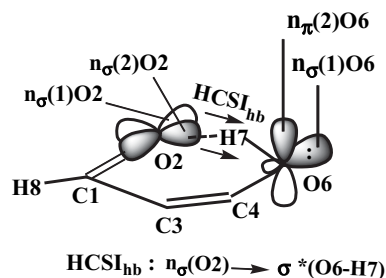


**Chart 4.** Labeling of the lone pair orbitals on O2 and O6. HCSI<sub>hb</sub> signifies the HB donor–acceptor hyperconjugative SIs (from the O2 lone pairs to the O6–H7 antibond orbital)

**Table 5.** Charge transferred ( $\Delta Q$ ), NBO second-order interaction energy ( $E(2)$ ) and the associated parameters for the donor-acceptor interactions (NBOs(i)  $\rightarrow$   $\sigma^*(\text{O6-H7})(j)$ ), O-H and O...H distances, and O-H and O...H NBO bond orders (in square brackets) calculated at the B3LYP/6-311++G(d,p) level

	$R_{\text{O}\cdots\text{H}}$ (Å)	$R_{\text{O-H}}$ (Å)	Donor NBO(i)	$\Delta Q$ (e)	$\Delta Q_{ij}$ (e)	$-E(2)$ (kcal/mol)	$E_j - E_i$ (a.u.)	$F_{ij}$ (a.u.)
<b>I</b>	1.703	0.997	$n_{\sigma}(1)\text{O2}$	0.063	0.0050	3.39	1.07	0.054
	[0.091]	[0.581]	$n_{\sigma}(2)\text{O2}$	(0.057)	0.0474	20.23	0.68	0.107
<b>I'</b>			$\sigma$ (C3-C4)	0.0020		1.48	1.16	0.037
<b>Ib</b>	1.651	1.002	$n_{\sigma}(1)\text{O2}$	0.073	0.0059	3.93	1.07	0.058
	[0.110]	[0.568]	$n_{\sigma}(2)\text{O2}$	(0.0674)	0.0582	25.21	0.69	0.119
<b>Ib'</b>			$\sigma$ (C3-C4)	0.009		1.94	1.14	0.042
<b>IIb</b>	1.514	1.040	$n_{\sigma}(1)\text{O2}$	0.117	0.0095	5.90	0.99	0.070
	[0.179]	[0.520]	$n_{\sigma}(2)\text{O2}$	(0.127)	0.1135	47.01	0.66	0.160
<b>IIb'</b>			$\sigma$ (C3-C4)	0.0027		1.98	1.15	0.043
<b>IIIb</b>	1.550	1.028	$n_{\sigma}(1)\text{O2}$	0.105	0.0085	5.40	1.01	0.067
	[0.158]	[0.533]	$n_{\sigma}(2)\text{O2}$	(0.107)	0.0946	39.77	0.67	0.148
<b>IIIb'</b>			$\sigma$ (C3-C4)	0.0028		2.07	1.16	0.044

<sup>a</sup> $\Delta Q_{ij}$  values are derived quantities from use of relations given in Ref. 30;  $E_i$ ,  $E_j$ ,  $F_{ij}$  have the usual meaning given therein;  $\Delta Q$  values (no parenthesis) are occupancies of the  $\sigma^*(\text{O6-H7})$  antibonds and  $\Delta Q$ 's in parentheses are the sum  $\sum \Delta Q_{ij}$ . The  $\sigma^*(\text{O6-H7})$  occupancies in the cO forms are: 0.00849 e (**IIb**); 0.0099 e (**IIIb**); 0.00909 e (**Ib**); and 0.00564 e (**I**). Primes indicate the non-H-bonded (cO) forms. Results are from B3LYP/6-311++G(d,p) calculations.

designated as  $E(2)_{2\text{O}2}$  hereafter). To determine if  $E(2)_{2\text{O}2}$  correlates with the apparent IMHB energy  $E_{\text{HB,A}}$ , the degree to which the  $E_{\text{HSE}}$ s and the  $E_{\text{HBE}}$ s correlate with the  $E(2)_{2\text{O}2}$  data has been tested. Table 6 presents the relevant parameters.

Let us first consider the case of  $E_{\text{HSE}}$ .<sup>110</sup> Figure 9A shows a plot of  $E_{\text{HSE}}$  versus  $E(2)_{2\text{O}2}$ . The plot also includes  $E_{\text{NSE}}$  data (differences in energy obtained via Eqn (1)) for **IIb**, **IIIb**, **Ibc**, **IIIbc**, and **V**. Clearly, the  $E_{\text{NSE}}$  data deviate from the trend. The  $E_{\text{NSE}}$  values for these systems have been identified as anomalous in earlier sections. The plot is, therefore, consistent with our previous findings already discussed. However, the trend for the other systems shows an excellent correlation, and the equation found is

$$E_{\text{HSE}} = 0.395E(2)_{2\text{O}2} - 5.167 \quad (8)$$

$[R = 0.992; n = 11 \text{ (data points)}; S_{\text{D}} = 0.346]$

Figure 9B shows a plot of  $E_{\text{HBE}}$  and  $E_{\text{HSE}}$  versus  $E(2)_{2\text{O}2}$ . In this case,  $E_{\text{HBE}}$ s are used instead of  $E_{\text{NSE}}$ s for the five

systems that deviated in Fig. 9A [for the 11 systems of Eqn (8),  $E_{\text{HBE}} \cong E_{\text{HSE}}$ ]. It is evident from the plot that system **V** (and may be **IIIac** as well) shows some deviation. The deviation, at least in the case of **V**, is due to the predicted  $E_{\text{HBE}}$  being  $-15.5$  kcal/mol when it should be of the order of  $-13.6$  kcal/mol, as discussed in Natural Bond Orbital Studies section. Nevertheless, the correlation is of high degree of fidelity even with the two data points included and the following equation was found.

$$E_{\text{HBE}} = 0.325E(2)_{2\text{O}2} - 6.643 \quad (9)$$

$[R = 0.974; n = 16 \text{ (data points)}; S_{\text{D}} = 0.813]$

If the data points for **V** and **IIIac** are excluded, the following equation obtains and the correlation is actually excellent.

$$E_{\text{HBE}} = 0.332E(2)_{2\text{O}2} - 6.272 \quad (10)$$

$[R = 0.991; n = 14 \text{ (data points)}; S_{\text{D}} = 0.487]$

**Table 6.** Second-order interaction energies  $E(2)^a$  and apparent HB energies estimated in an empirical manner ( $E_{\text{HB,E}}$ )<sup>b,c</sup> (both in kcal/mol) for MAE derivatives with O...H-O IMHB motifs. Values in parentheses are  $\Delta E_{\text{SE,S}}$ .

$S^d$	$-E(2)$	$-E_{\text{HB,E}}$	$S^e$	$-E(2)$	$-E_{\text{HB,E}}$	$S^f$	$-E(2)$	$-E_{\text{HB,E}}$
<b>I</b>	20.2	13.3 (13.3)	<b>I</b>	20.2	13.3 (13.3)	<b>I</b>	20.2	13.3 (13.3)
<b>Ia</b>	21.3	14 (13.4)	<b>IIa</b>	15.6	11 (10.9)	<b>IIIa</b>	18.3	12.7 (12.1)
<b>Ib</b>	25.2	14.7 (15.1)	<b>IIb</b>	47	21.1 (14.5)	<b>IIIb</b>	39.8	19.6 (13.4)
<b>Ic</b>	22.9	14.1 (14.4)	<b>IIc</b>	10.6	9.4 (10.1)	<b>IIIc</b>	10.5	9.4 (9.3)
<b>Ibc</b>	27.3	15.6 (16.2)	<b>IIac</b>	8.9	8.4 (8.7)	<b>IIIac</b>	13.2	12 (10)
<b>V</b>	20.8	15.5 (9.2)	<b>IIbc</b>	15.9	12 (9.7)	<b>IIIbc</b>	16.5	12.1 (8.5)

<sup>a</sup>Results are from B3LYP/6-311++G(d,p).

<sup>b</sup>Results are from B3LYP/6-311G(d,p) calculations.

<sup>c</sup> $E_{\text{HB,E}}$ s are those estimated using the regression function for the  $E_{\text{HSE}}-R(\text{O}\cdots\text{O})$  correlation.

<sup>d</sup>Molecular systems. Methyl derivatives except for system **V** (see Chart 1).

<sup>e</sup>Molecular systems. F derivatives.

<sup>f</sup>Molecular systems. Cl derivatives.

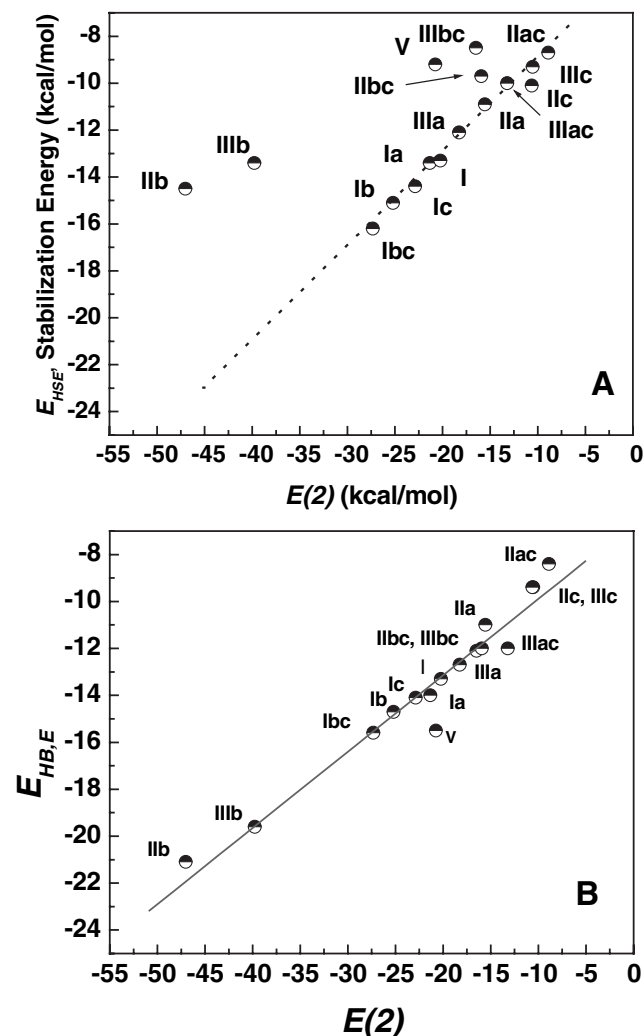


**Figure 9.** A: Scatter plot of  $E_{HSE}$  against  $E(2)_{2O_2}$  [ $E(2)$  of the  $n_{\sigma^2}(O_2) \rightarrow \sigma^*(O-H)$  SI]. B: Correlation of  $E_{HB,E}$  with  $E(2)_{2O_2}$ . In this figure, Subpart B is to be compared with subpart A. The deviation seen for **V** is because Eqn (2) overestimates its  $E_{HB,E}$  (owing to the artificial contraction of the  $O \cdots O$  distance as explained in the text)

Three important conclusions emerge from the correlated behavior observed in Fig. 9. (1)  $E(2)_{2O_2}$  does correlate with both  $E_{HSE}$  and  $E_{HB,E}$ , and hence it can be concluded that it correlates with the apparent IMHB energy,  $E_{HB,A}$  as well. (2) The behavior provides strong evidence that some of the energy differences calculated by Eqn (1) ( $E_{HSE}$ s) can indeed serve as measures of the HB strength. (3) The behavior also serves as supporting evidence for the validity of the exponential  $E_{HSE}-R(O \cdots O)$  correlation (Trend in Energetic ( $E$ ) Versus Geometrical ( $G$ ) Consequences section).

The NBO study also showed that the F and Cl  $\beta$ -substituents enhance, and augment, the D-A ability of the main  $\pi$  conjugative SIs (data not shown), but dramatically enhance the  $n_{\sigma^2}(O_2) \rightarrow \sigma^*(O-H)$  SIs. By contrast, single (double) substitution(s) at  $\alpha$ - and carbonyl position(s)

generally diminish the dominant  $n_{\sigma^2}(O_2) \rightarrow \sigma^*(O-H)$  SI. In the methyl case, substitutions at all positions lead to enhancement. More detailed analyses of all aspects of the effects of substituents at different positions are not within the scope of this paper, and may be addressed in future communications.

## SUMMARY AND CONCLUSIONS

A detailed study of the energetic, geometrical, and electronic consequences of H bonding has been made. Through the use of known experimental values of energies of HB formation, the electronic consequences of H bonding and other measures of HB strength, the separation of the classically computed energetic parameters ( $\Delta E_{SES}$ ) into (i) stabilization (HB) energies ( $E_{HSE}$ s) that serve as apparent IMHB energies ( $E_{HB,AS}$ ), and (ii) stabilization (isomerization) energies ( $E_{NSE}$ s) that do not (owing to intractable interactions that are not germane to the solitary HB donor(D)-acceptor(A) interactions) has been accomplished. The sources of the intractable interactions have been rationalized. The study shows the  $O \cdots O$  distance ( $G$  consequence) is, with some exceptions, a reliable indicator of IMHB strength.

Analysis of the energetic-geometrical ( $E \leftrightarrow G$ ), that is,  $E_{HSE}-R(O \cdots O)$  trend led to both an exponential and a quadratic model. The exponential model is consistent with the fundamental behavior (e.g., asymptotic behavior) of the  $E \leftrightarrow G$  correlation of intermolecular HBs. By contrast, the quadratic model found for  $E_{HSE}-R(O \cdots O)$  correlation was found to be unphysical. The exponential model also has *predictive ability*, and can be used to make reasonable estimates of  $E_{HB,AS}$  that are otherwise grossly underestimated. The model can also be used to treat RAHBs whose resonant spacers connecting the HB D-A segments are very different. The study also shows that the HB strengths of NZ and MAE are essentially the same (despite the different nature of resonant spacers).

AIM and NBO approaches allow the isolation of the HB D-A interactions from intractable interactions that are not germane to the HB interaction. Accordingly, the electronic consequences of H bonding have been used to check if the quantum chemically calculated HB SEs are acceptable measures of the HB strength and to obtain reliable relative HB strengths. Hence, the AIM and NBO approaches can serve as complementary, and sometimes indispensable, alternatives for the calibration and rationalization of IMHB strengths, and are highly recommended especially for the study of IMHBs, which may involve intractable interactions.

## Supplementary material available

Two figures along with discussion text on the assessment of the causes of the intractable interactions. This

material is available free of charge via the Internet at <http://www.interscience.wiley.com/jpages/0894-3230/suppmat/>

## Acknowledgements

This work was supported by HHS/MBRS/SCORE Program, Grant No. S06-GM08247. This work has also benefited from the financial support for computer and software maintenance by a grant from NSF/MRCE (Grant No. HRD-915407).

## REFERENCES

- (a) Pimentel GC, McClellan AL. *The Hydrogen Bond*. Freeman: San Francisco, CA, 1960 (Supplemental 1971); (b) Emsley J. *Struct. Bond.* 1984; **57**: 147; (c) Jeffrey GA, Saenger W. *Hydrogen Bonding in Biological Structures*. Springer-Verlag: Berlin, 1991; (d) Jeffrey GA. *An Introduction to Hydrogen Bonding*. Oxford University Press: New York, 1997.
- Gordon MS, Jensen JH. *Acc. Chem. Res.* 1996; **29**: 536.
- Aquino JA, Tunega D, Haberhauer G, Gerzabeck MH, Lischka H. *J. Phys. Chem. A* 2002; **106**: 1862, and references therein.
- Hobza P, Sponer J. *Chem. Rev.* 1999; **99**: 3247.
- Kirby AJ. *Acc. Chem. Res.* 1997; **30**: 290.
- (a) Dupre DB, Yappert MC. *J. Phys. Chem. A* 2002; **106**: 567; (b) Mishra SK, Mishra PC. *J. Comput. Chem.* 2002; **23**: 530; (c) MÓ O, Yáñez M. *J. Phys. Chem. A* 1998; **102**: 8174; (d) Dkhissi A, Adamowicz L, Maes G. *J. Phys. Chem. A* 2000; **104**: 2112; (e) Schlucker S, Singh RK, Asthana BP, Popp J, Kiefer W. *J. Phys. Chem. A* 2001; **105**: 9983.
- (a) Ricca A, Bauschlicher CW., Jr. *J. Phys. Chem. A* 2002; **106**: 3219; (b) Mmercki BT, Donaldson DJ. *J. Phys. Chem. A* 2002; **106**: 185.
- (a) Bertran DN, Onuchlic HN. *Photosynthesis Res.* 1989; **22**: 173; (b) Bertran DN, Onuchlic HN. *Science* 1991; **252**: 1285; (c) Onuchlic HN, Bertran DN, Winkler JR, Gray HB. *Annu. Rev. Biophys. Biomol. Struct.* 1992; **21**: 349; (d) Wuttke DS, Bjerrum MJ, Winkler JR, Gray HB. *Science* 1992; **256**: 1007.
- Chou P-T, Wei C-Y, Wang C-RC, Hungand F-T, Chang C-P. *J. Phys. Chem. A* 1997; **101**: 9496.
- Acton EM. In *Anthracycline Antibiotics*, Priebe W (ed.). *ACS Symposium Series 574*, American Chemical Society: Washington, DC, 1995.
- Tong GL, Henry DW, Acton EM. *J. Med. Chem.* 1979; **22**: 36.
- Myers CE, Muinda JRF, Zweier J, Sinha BK. *J. Biol. Chem.* 1987; **262**: 11571, and references therein.
- Lown JW, Chen HH, Plambeck JA. *Biochem. Pharma.* 1979; **28**: 2563.
- (a) Mariam YH, Chantranupong L, Niles J. *J. Mol. Struct. (Theochem)* 1999; **487**: 127; (b) Mariam YH, Musin RN. *J. Mol. Struct. (Theochem)* 2001; **549**: 123–136.
- (a) Seliskar CJ, Hoffmann RE. *J. Mol. Spectros.* 1982; **96**: 146; (b) Smith Z, Wilson EB, Duerst RW. *Spectrochim. Acta.* 1983; **39A**: 1117; (c) Krokidis X, Goncalves A, Savin A, Silvi B. *J. Phys. Chem.* 1985; **102**: 5065; (d) Binkley JS, Frisch MJ, Schaefer HF, III. *Chem. Phys. Lett.* 1986; **126**: 1; (e) Sim F, St-Amant A, Papai I, Salahub DR. *J. Am. Chem. Soc.* 1992; **114**: 4391, and references therein; (f) Wolf K, Mikenda W, Nustere E, Schwartz K. *J. Mol. Struct.* 1997; **448**: 201; (g) Perrin CL, Kim Y-J. *J. Am. Chem. Soc.* 1998; **120**: 12641; (h) Boese R, Antipin MY, Bläser D, Lyssenko KA. *J. Phys. Chem. A.* 1998; **102**: 8654 and references therein; (i) Mavri J, Grdadolnik J. *J. Phys. Chem. A.* 2001; **105**: 2045; (j) Rios MA, Rodriguez J. *J. Mol. Struct. (Theochem).* 1990; **204**: 137–144 (and references therein for both experimental and theoretical studies on AAE); (k) Coe JD, Martinez TJ. *J. Am. Chem. Soc.* 2005; **127**: 4560–4561; (l) Aquino AJA, Lischka H, Hättig C. *J. Phys. Chem. A.* 2005; **109**: 3201–3208; (m) Gora RW, Grabowski SJ, Leszczynski J. *J. Phys. Chem. A.* 2005; **109**: 6397–6405; (n) Özen AS, De Proft F, Aviyente V, Geerlings P. *J. Phys. Chem. A.* 2006; **110**: 5860–5868.
- (a) Although the effect of  $\pi$  conjugation on the strength of H bonding has been reported before from an experimental perspective,<sup>16b</sup> it was Gilli's group that first introduced the resonance-assisted (RA) HB (RAHB) model<sup>17</sup> to rationalize the nature of the strong IMHB in typical  $\beta$ -diketone enols; (b) Kopteva TS, Shigorin DN. *Russ. J. Phys. Chem.* 1974; **48**(3): 312–314, and references therein.
- (a) Gilli G, Bellucci F, Ferretti V, Bertolasi V. *J. Am. Chem. Soc.* 1989; **111**: 1023; (b) Bertolasi V, Gilli P, Ferretti V, Gilli G. *J. Am. Chem. Soc.* 1991; **113**: 4917; (c) Gilli P, Bertolasi V, Ferretti V, Gilli G. *J. Am. Chem. Soc.* 1994; **116**: 909. (d) Gilli P, Ferretti V, Bertolasi V, Gilli G. In *Advances in Molecular Structure Research*, vol. 2, Hargittai I, Hargittai M (Eds). JAI Press Inc: Greenwich, CT, 1996; 67–102.
- In the Gilli group initial study,<sup>17a</sup> only selected molecular systems were included in the analyses to avoid, according to the authors, "unwanted geometry perturbations".<sup>19</sup> Some of the cases excluded were fragments where the C<sub>a</sub>, C<sub>b</sub> or C<sub>c</sub> atoms (Chart 1) were part of an aromatic ring. As a result, at least in the case of the NZ type systems, the RAHB Q parameter may not be envisioned to be applicable for assessing the strength of the HBs.
- (a) The differences may be expected to lead to different  $\pi$  electron delocalization, dipolar field/inductive and polarizability effects;<sup>19b</sup> (b) Taft RW, Koppel LA, Topson RD, Aniva F. *J. Am. Chem. Soc.* 1990; **112**: 2047.
- Espinosa E, Molins E, Lecomte C. *Chem. Phys. Lett.* 1998; **285**: 170. This paper discusses the exponential dependence of the HB interaction energy on the HB distance for the intermolecular case.
- For example: (1) In typical  $\beta$ -diketone enols, it has been shown that experimental O—H bond lengths are good descriptors of IMHB strength.<sup>22</sup> A linear correlation between O—H covalent bond lengths and IMHB energy has also been reported for the case of 2-hydroxybenzoyl compounds by Palomar *et al.*<sup>22</sup> (2) O...O and O...H distances (respectively, R(O...O) and R(O...H)) have been found to be proportional to the three mutually inter-related parameters that have been used to characterize the strength of HBs: O—H bond lengths,  $\nu$ (O—H) stretching frequencies and O—H chemical shifts  $\delta_{\text{O—H}}$ . Accordingly, O...O and O...H distances have been shown to be adequate parameters for "quantifying" the HB interaction.<sup>17,22</sup> (3) The strength of RAHBs, as estimated by O...O and O...H distances, has also been shown to correlate with the  $\pi$  electron delocalization as estimated by the so-called Q parameter.<sup>17</sup> (4) For some F and Cl derivatives of MAE, three quadratic correlations: (i) HB energy—O...H distance; (ii) HB energy— $\rho_b$ (charge density at the HB bond critical point); and (iii) HB energy—Q parameter have been reported.<sup>23</sup> (5) The dependence of HB energy on a proposed complex parameter, based on the geometrical and topological parameters of the O—H bond, was also reported, and the dependence was found to be nonlinear (quadratic) in the case of IMHBs, and linear in the case of intermolecular HBs.<sup>24</sup>
- Palomar J, De Paz JLG, Catalán J. *J. Phys. Chem. A.* 2000; **104**: 6453, and references therein.
- Grabowski SJ. *J. Molec. Struct.* 2001; **562**: 137–143.
- Grabowski SJ. *J. Phys. Chem. A* 2001; **105**: 10739–10746.
- In contrast to the observations summarized in Ref. 21: (1) It has been observed that O...O distances may not always be genuine indicators of the HB strength because they can be sometimes thrust together by steric, electronic or other constraints.<sup>26</sup> (2) In 2-hydroxybenzoyl compounds, calculated at the B3LYP/6-31G\*\* level, O—H bond lengths showed a linearly correlated behavior with IMHB energy, but O...O and O...H distances showed a worse correlation with IMHB energy.<sup>22</sup> (3) Korth *et al.*<sup>27</sup> had investigated a series of 2-substituted phenols, and found generally poor correlation between the IMHB enthalpy and geometrical factors such as R(O—H) and R(OH...A), where A is the HB accepting atom. (4) Grabowski has proposed that the HB may be better characterized by incorporating the van der Waals radii of the donor and acceptor atoms in the correlation of the inter- and intramolecular HB energy.<sup>24</sup> But, the Korth *et al.*<sup>27</sup> group did not find any improvement when they analyzed their data in accordance to this approach.

26. Buemi G, Zuccarello F. *Electron. J. Theor. Chem.* 1997; **2**: 302–314 and references therein.
27. Korth H-G, de Heer MI, Mulder P. *J. Phys. Chem. A.* 2002; **106**: 8779.
28. Korth H-G, de Heer MI, Mulder P. In fact suggest such an attempt is destined to fail. As a possible explanation for those instances for which  $E \leftrightarrow G$  correlations have been reported,<sup>23,24</sup> they observed that correlations of IMHB enthalpy with a single or multiple geometrical parameter(s) may only be appropriate within a small family of compounds where the (structural) perturbation may be assumed to be rather constant.
29. Bader RFW. *Atoms in Molecules: A Quantum Theory*. Oxford University Press: New York, 1994.
30. (a) Foster JP, Weinhold FA. *J. Am. Chem. Soc.* 1980; **102**: 7211; (b) Reed AE, Weinstock RB, Weinhold FA. *J. Chem. Phys.* 1985; **83**: 735; (c) Reed AE, Curtiss A, Weinhold F. *Chem. Rev.* 1988; **88**: 899; (d) Weinhold F, Carpenter JE. In *The Structure of Small Molecules and Ions*, Naaman R, Vager Z (eds). Plenum: New York, 1988; pp. 227–236.
31. (a) Becke AD. *J. Chem. Phys.* 1993; **98**: 5648; (b) Becke AD. *J. Chem. Phys.* 1992; **96**: 2155; (c) Becke AD. *J. Chem. Phys.* 1992; **97**: 9173; (d) Hehre WJ, Radom L, Schleyer PR, Pople JA. *Ab initio Molecular Orbital Theory*. Wiley: New York, 1986.
32. Some of the reasons and rationale that led to the choice of the B3LYP/6-311G(d,p) model include: (a) for the description of intermolecular HBs, the B3LYP model<sup>30a,33</sup> has been shown to give results in good agreement with high level *ab initio* calculations;<sup>34–37</sup> (b) the B3LYP/6-311G(d,p) model has been shown to give geometrical results that are in good accord with experiment;<sup>38,39</sup> (c) Barone and Adamo<sup>40</sup> had conducted an extensive study on MAE at several very high levels of theory and had found the B3LYP/6-311G(d,p) model to be a good compromise between accuracy of calculation and computational cost; (d) Schiøtt *et al.*<sup>41</sup> have also reported results that were in good accord with experiment. A report<sup>42</sup> from our laboratories which compared B3LYP/6-311G(d,p) results on MAE and NZ with those experimentally determined for MAE<sup>43</sup> and for NZ,<sup>44</sup> and those calculated for MAE<sup>45</sup> has confirmed the findings by other workers.<sup>38,39,45</sup>
33. Lee C, Yang W, Parr RG. *Phys. Rev. B.* 1988; **37**: 785.
34. Sim F, St-Amant A, Papai I, Salahub DR. *J. Am. Chem. Soc.* 1992; **114**: 4391.
35. González L, Mó O, Yáñez M. *J. Phys. Chem. A.* 1997; **101**: 9710, and references therein.
36. Lozynski M, Rusinka-Raszak D, Mack H-G. *J. Phys. Chem. A.* 1998; **102**: 2899.
37. Novoa JJ, Sosa C. *J. Phys. Chem.* 1995; **99**: 15837.
38. Mebel AM, Morokuma K, Lin CM. *J. Chem. Phys.* 1995; **103**: 7414.
39. Gu J, Leszczynski J. *J. Phys. Chem. A* 1999; **103**: 577.
40. Barone V, Adamo C. *J. Chem. Phys.* 1996; **105**: 11007.
41. (a) Schiøtt B, Iversen BB, Madsen GKH, Bruice TC. *J. Am. Chem. Soc.* 1998; **120**: 12117–12124; (b) Madsen GKH, Iversen BB, Larsen FK, Kapon M, Reisner GM, Herbststein FH. *J. Am. Chem. Soc.* 1998; **120**: 10040–10045.
42. Mariam YH, Chantranupong L. *J. Mol. Struct. (Theochem)*. 2000; **529**: 83.
43. Baughcum SL, Duerst RW, Rowe WF, Smith Z, Wilson EB. *J. Am. Chem. Soc.* 1983; **103**: 6296.
44. Tomioka Y, Ito M, Mikami N. *J. Phys. Chem.* 1983; **87**: 4401.
45. Frisch MJ, Scheiner AC, Schaefer III HF. *J. Chem. Phys.* 1995; **82**: 4194.
46. (a) Gaussian 98, Revision D.1, Frisch MJ, Trucks GW, Schlegel HB, Scuseria GE, Robb MA, Cheeseman JR, Zakrzewski VG, Montgomery JA, Stratman RE, Burant JC, Dapprich S, Millam JM, Daniels ADKudin KN, Strain MC, Farkas O, Tomasi J, Barone V, Cossi M, Cammi R, Mennucci B, Pomelli C, Adamo C, Clifford S, Ochterski J, Petersson GA, Ayala PY, Cui Q, Morokuma K, Malik DK, Rabuck AD, Raghavachari K, Foresman JB, Cioslowski J, Ortiz JV, Stefanov BB, Liu G, Liashenko A, Piskorz P, Komaromi I, Gomperts R, Martin RL, Fox DJ, Keith T, Al-Laham MA, Al-Laham MA, Peng CY, Nanayakkara A, Gonzalez C, Challacombe M, Gill PMW, Johnson BG, Chen W, Wong MW, Andres JL, Head-Gordon M, Replogle ES, Pople JA, Gaussian, Inc.: Pittsburgh, PA, 1998; (b) Gaussian 94, Revision D.1, was also used to a very limited extent.
47. Spartan 04, Wavefunction, Irvine, CA.
48. a) Popelier PLA. *Atoms in Molecules: An Introduction*. Pearson Education: Harlow, U. K., 2000. (b) Green ME. *J. Phys. Chem. A* 2002; **106**: 11221–11226.
49. Bader RFW, Tang TH, Tal Y, Biegler-König F. *J. Am. Chem. Soc.* 1982; **104**: 946.
50. (a) Gillespie RJ, Popelier PLA. *Chemical Bonding and Molecular Geometry: From Lewis to Electron Densities*, Oxford University Press: New York, 2001; (b) Heinemann C, Muller T, Apeloig Y, Schwarz H. *J. Am. Chem. Soc.* 1996; **118**: 2023.
51. (a) Bader RFW. *Acc. Chem. Res.* 1975; **8**: 34; (b) Bader RFW. *Chem. Rev.* 1991; **91**: 893; (c) Bader RFW, Popelier PLA, Keith TA. *Agnew. Chem.* 1994; **106**: 647; (d) Bader RFW, Gillespie RJ, MacDougall PJ. *J. Am. Chem. Soc.* 1988; **110**: 7329; (e) Bader RFW, Gillespie RJ, MacDougall PJ. In *Molecular Structure and Energetics*, vol. 11, Liebman JF, Greenberg A (eds). VCH: New York, 1989; (f) Bader RFW, Popelier PLA, Chang C. *J. Mol. Struct. (Theochem)* 1992; **87**: 145; (g) Bader RFW, Johnson S, Tang T-H, Popelier PLA. *J. Phys. Chem.* 1996; **100**: 15398.
52. (a) Biegler-König F, Bader RFW, Tang TH. *J. Comput. Chem.* 1982; **13**: 317; (b) Biegler-König F, Schönbohm J, Bayles D. *J. Comput. Chem.* 2001; **22**: 545.
53. (a) Buemi G, Zuccarello F. *J. Chem. Soc., Faraday Trans.* 1996; **92**: 347; (b) Buemi G, Zuccarello F. *Electron. J. Theor. Chem.* 1997; **2**: 118; (c) Buemi G. *Chem. Phys.* 2002; **277**: 241–256.
54. Chen C, Chang CW, Wang YM. *J. Molec. Struct. (THEOCHEM)*. 1994; **311**: 19–28.
55. Stephens PJ, Devlin FJ, Chabalowski CF, Frisch MJ. *J. Phys. Chem.* 1994; **98**: 11623.
56. (a) Gilli P, Bertolasi V, Ferretti V, Gilli G. *J. Am. Chem. Soc.* 2000; **122**: 10405; (b) Gilli G, Gilli P. *J. Mol. Struct.* 2000; **552**: 1.
57. (a) González L, Mó O, Yáñez M. *J. Phys. Chem. A.* 1997; **101**: 9710, and references therein; (b) Marvi J, Grdadolnik JJ. *Phys. Chem. A.* 2001; **105**: 2039.
58. Egan W, Gunnarsson G, Bull TE, Forsen S. *J. Am. Chem. Soc.* 1977; **99**: 4568–4572.
59. Dannenberg JJ, Rios RJ. *J. Phys. Chem. A* 1994; **98**: 6714.
60. Buemi and Zuccarello<sup>53b</sup> have compared results for **I** and **Ibc** obtained from use of MP2/6-31G\*\* and B3LYP/6-31G\*\* models, and they concluded that both the MP2/6-31G\*\* and B3LYP/6-31G\*\* results fit experimental data on these systems sufficiently.
61. (a) Busch JH, Fluder EM, de la Vega JR. *J. Am. Chem. Soc.* 1980; **102**: 4000; (b) Ogoshi H, Yoshida Z. *Chem. Commun.* 1970; 176; (c) Iijima K, Onhogi A, Shibata S. *J. Mol. Struct.* 1987; **156**: 111; (d) both the MP2/6-311++G(d,p) and B3LYP/6-311G(d,p) O...O distances (respectively 2.584 and 2.582 Å), which differ from each other by 0.002 Å, are longer than the experimental 2.553 Å value reported for **I**.<sup>43</sup> With regard to the O...H distance for **I**, again both methods give longer distances (respectively 1.686 and 1.69 Å) compared to the experimental value of 1.68 Å.<sup>43</sup> In the case of **Ibc**, the MP2/6-311++G(d,p) and B3LYP/6-311G(d,p) O...O distances (respectively 2.549 and 2.543 Å), which differ by 0.006 Å, are considerably longer than the 2.512 and 2.538 Å values reported.<sup>59,61b</sup> On the other hand, they both are in excellent agreement with the experimental value of 2.547 Å reported by Boese *et al.*<sup>15h</sup> and the theoretical value of 2.549 Å reported by Dannenberg and Rios at the MP2/D95++ level.<sup>59</sup> Interestingly enough, a very recent result from Zewail's group<sup>61c</sup> puts the O...O distance at 2.592 Å making both the MP2 and B3LYP O...O distances considerably shorter, and the other experimental O...O distances of 2.38 and 2.512 Å too short; (e) Srinivasan R, Feenstra JS, Park ST, Xu S, Zewail AH. *J. Am. Chem. Soc.* 2004; **126**: 2266–2267, and references therein.
62. (a) Palomar J, De Paz JLG, Catalán J. *J. Phys. Chem. A.* 2000; **104**: 6453–6463; (b) Chung G, Kwon O, Kwon Y. *J. Phys. Chem. A.* 1997; **101**: 9415; (c) Rodriguez-Santiago L, Sodupe M, Oliva A, Bertran J. *J. Am. Chem. Soc.* 1999; **121**: 8882–8890; (d) Catalán J, Palomar J, De Paz JLG. *J. Phys. Chem. A.* 1997; **101**: 7914–7921; (e) Lampert H, Mikenda W, Karpfen A. *J. Phys. Chem. A.* 1996; **101**: 7418–7425; (f) Rabuck AD, Scuseria GE. *Theo. Chem. Acc.* 2000; **104**: 438. The report by Gávanéz and Gómez also supports this view;<sup>62g</sup> (g) Gávanéz O, Gómez PC, Pacios LF. *J. Chem. Phys.* 2001; **115**: 11166–11184.

63. (a) Hibbert F, Emsley J. *J. Adv. Phys. Org. Chem.* 1990; **26**: 255; (b) Alkorta I, Elgeuro J. *J. Phys. Chem. A* 1999; **103**: 272–279.
64. Madsen GKH, Wilson C, Nymad TM, McIntyre GJ, Larsen FK. *J. Phys. Chem. A* 1999; **103**: 8684–8690, and references therein.
65. On the basis of the energetic parameter, one would also be led to conclude the HB strengths of **I**, **IIb** and **IIIb** are weaker than that of **Ibc**. But, since the O...O distances for **I**, **IIb** and **IIIb** (Table 2) are significantly different from each other, the calculated geometrical consequences strongly suggest the HB strengths in the three systems should be necessarily very different.
66. (a) Dannenberg JJ, Rios RJ. *J. Phys. Chem. A* 1999; **103**: 7083 (and references therein); (b) References 1b and 17a.
67. References 15j, 16b, 58 and references therein.
68. **IIb** and **IIIb** were two of the systems included in the parametric quadratic model reported in references 23 and 24. But, the estimate of the error (up to 10 kcal/mol or so) in the calculated HB stabilization energies for these systems does not suggest that the quadratic model in the Grabowski reports<sup>23,24</sup> would be applicable even to the small family of systems considered as suggested by Korth *et al.*<sup>27</sup>
69. (a) Bader RFW, Slee TS, Cremer D, Kraka E. *J. Am. Chem. Soc.* 1983; **105**: 5061–5068; (b) Cremer D, Kraka E, Slee TS, Bader RFW, Lau CDH, Nguyen-Dang TT, MacDougall PJ. *J. Am. Chem. Soc.* 1983; **105**: 5069–5075.
70. (a) Gordon AJ, Ford RA. *The Chemist's Companion*. John Wiley & Sons: New York, NY: 1972, p. 109; (b) The question of whether the H...F and H...Cl interactions can be characterized as IMHBs (respectively, O—H...F and O—H...Cl) or not has been considered using the AIM approach.<sup>20</sup> To answer this question, one has to find a hydrogen bond critical point (HBCP).<sup>48,70c,d</sup> However, the search for such an HBCP (and a bond path (BP) connecting the H and the F/Cl atoms) using the default stepsize settings (0.1) of the AIM2000 program<sup>52a</sup> was not successful. Further attempts to find the critical points sought by reducing the stepsize to even 0.01 x default was not helpful either. This result strongly suggests that the H...F and H...Cl interactions may not be characterized as HBs. Consequently the interactions have to be due to van der Waals forces; (c) Koch U, Popelier PLA. *J. Phys. Chem.* 1995; **99**: 9747–9754; (d) Popelier PLA. *J. Phys. Chem.* 1998; **102**: 1873–1878.
71. (a) Pross A, Radom L. *Prog. Phys. Org. Chem.* 1981; **13**: 1; (b) Apeloig Y, Karmi M. *J. Am. Chem. Soc.* 1980; **106**: 6676; (c) Slee TS, Larouche A, Bader RFW. *J. Phys. Chem.* 1988; **92**: 6219; (d) Libit L, Hoffman R. *J. Am. Chem. Soc.* 1974; **97**: 1370.
72. Furthermore, Libit and Hoffman<sup>71d</sup> had proposed that substituent  $\pi$  effects could also involve polarization of the adjacent  $\pi$  system. In other words, in the present case, the F, Cl, and CH<sub>3</sub> substituents at the  $\beta$  position can polarize the C3=C4 bond (push  $\pi$  density from atom C4 to C3)<sup>71c</sup> thereby elongating the bond to some extent. Hence, the inequality  $|E_{SE}| < |E_{HB,A}|$  may be partly a manifestation of (a) destabilizing effects, upon H bonding, due to  $\sigma$  electron delocalization that differ in magnitude in different systems, and (b) varying degrees of polarization effects in the cO and cC forms.
73. Alabugin IV, Manoharan M, Peabody S, Weinhold F. *J. Am. Chem. Soc.* 2003; **125**: 5973, and references therein.
74. Hoppe W, Lohmann W, Karkl H, Ziegler H (eds). *Biophysics*. Springer-Verlag: New York, 1983; p.226
75. (a) A plot of  $\rho_b$  (at O—H BCP) versus  $R_{O-H}$  should provide essentially the same kind of information as the plot of  $\rho_{bH}$  against the O...H distance;<sup>75b-f</sup> (b) Rozas I, Alkorta I, Elgeuro J. *J. Am. Chem. Soc.* 2000; **122**: 11154; (c) Grabowski SJ. *J. Phys. Org. Chem.* 2004; **17**: 18–31; (d) Grabowski SJ. *Monatsh. Chem.* 2002; **133**: 1373–1380; (e) Wojtulewski S, Grabowski SJ. *J. Mol. Struct.* 2003; **645**: 287–294; (f) Wojtulewski S, Grabowski SJ. *J. Mol. Struct. (Theochem)* 2003; **621**: 285–291.
76. (a) The same quasilinear regression line ( $\rho_{b,O-H} = -7.7R_e + 9.88$ ,  $R^2 = 0.994$ ) can fit all the data points (with a very good correlation); (b)  $\rho_b$  is a reasonable measure of the strength of a bond,<sup>70b,77</sup> meaning the stronger (weaker) the bond, the greater (lower) the  $\rho_b$ . The result obtained here is consistent with this electron density-bond length relationship.<sup>76c-e,77a</sup> This behavior of  $\rho_b$  is thought to be similar to that of the Coulson's (Coulson, C. A. *Proc. R. Soc. London, Ser. A* **1939**, 169, 413) bond order parameter;<sup>76c-e</sup> (c) Roversi P, Barzaghi M, Merati F, Destro R. *Can. J. Chem.* 1996; **74**: 1145; (d) Knop O, Rankin KN, Boyd RJ. *J. Phys. Chem. A* 2001; **105**: 6552; (e) Luaña V, Pendás AM, Costales A, Carriedo GA, Garcia-Alonso FJ. *J. Phys. Chem. A* 2001; **105**: 5280 and references therein.
77. (a) Bader RFW, Tang TH, Tal Y, Biegler-König F. *J. Am. Chem. Soc.* 1982; **104**: 946; (b) Wiberg KB, Bader RFW, Lau CDH. *J. Am. Chem. Soc.* 1987; **109**: 1001.
78. The decrease in  $\rho_b$  with the increase in the elongation of the O—H bonds can also be interpreted as showing the increase in the polarization of the O—H bonds paralleling the increase in the HB strength.<sup>74</sup>
79. There are three additional observations that should be noted about the R(G) and R( $\rho_b$ ) rankings. First, **IV** (o-hydroxy benzaldehyde)<sup>80</sup> is shown to be, by both the R(G) and R( $\rho_b$ ) rankings, substantially weaker than several systems including the prototypical  $\beta$ -diketones, i.e., **I** and **Ibc**. Second, **Ibc** should be stronger than **I** (and **Ib**)<sup>26</sup> and the R(G) and R( $\rho_b$ ) rankings are consistent with the reported findings. Third, system **V** (HOCR=N—CR=O)—in which the C=C and C—C bonds are replaced by C=N and C—N bonds—is found to be as strong or slightly stronger than **I** on the basis of its O...O distance and the AIM data. However, based on the Q parameter (Table 2) it falls near the bottom of the ranking.
80. (a) O-hydroxy benzaldehyde (**IV**) is one of the kinds of systems that was excluded in the study of the development of the RAHB model.<sup>17</sup> This system has been studied in detail.<sup>62c,80b</sup> Our results (such as O...O and O...H distances) are in good agreement with those reported in those studies; (b) Cuma M, Scheiner S, Kar T. *J. Mol. Struct. (Theochem)* 1999; **487**: 37–49.
81. The modulations include  $\pi$  electron conjugation superimposed on those of  $\sigma$ -electron delocalization, dipolar field/inductive and polarizability contributions, bond-length and bond-angle deformations, bond polarizations, O...O repulsions, and in the case of the halo derivatives, possibly O...F, O...Cl, Cl...Cl, F...F long-range repulsions as well.
82. The entries in Table 3 include: O...H HB distances  $R(O...H)$ ; topological consequences at the HBCP: the electron density  $\rho_b(O...H)$ ,  $V_b$  and  $H_b$ ; elongation of the O—H bonds ( $\Delta R$ ) and the corresponding harmonic (uncorrected) frequency shifts ( $\Delta \nu$  cm<sup>-1</sup>) of the O—H bonds (along with  $\Delta E_{SE}$ ,  $\rho_b$  at the BCP of the O—H bonds, Q, O...O distances from Table 2). The different entries are primarily for those systems (with O...H—O HB motifs) whose  $\Delta E_{SE}$  values as measures of the HB strengths are in question so that comparison of the various parameters with that for **I** and **Ibc** can easily be made.
83. The constellation of results in Table 3, when taken collectively show: (i) the trend in the HB strengths follows the suborder **IIb** > **IIIb** > **Ibc** > **Ib** > **I**. This suborder, while it is consistent with AIM and O...O orders discussed before, is not in agreement with the Q order. (ii) The HB strength of **V** is comparable to that of **I** and **Ia**, (iii) the HB strengths of **IIbc** and **IIIbc** are comparable to each other but slightly weaker than that of **I**, and (iv) the HB strengths of **IIa** and **IV** are also comparable to each other, but slightly weaker than that of **IIbc** and **IIIbc**.
84. (a) Gilli P, Bertolasi V, Pretto L, Lycka A, Gilli G. *J. Am. Chem. Soc.* 2002; **124**: 13554–13567; (b) Gilli P, Bertolasi V, Pretto L, Ferretti V, Gilli G. *J. Am. Chem. Soc.* 2004; **126**: 3845–3855; (c) Gilli P, Bertolasi V, Pretto L, Antonov L, Gilli G. *J. Am. Chem. Soc.* 2005; **127**: 4943–4953.
85. (a) The O...S and O...Se interatomic distances, respectively in **VI** and **VII**, were actually calculated to be shorter in the cO forms than those in the cC forms (The same obtains for O...N in **X** as well.) The shorter distances in the case of the non-hydrogen bonded forms of **VI** and **VII** are consistent with results reported before,<sup>85c-d</sup> and have been attributed to O...S and O...Se attractive forces. To confirm the B3LYP/6-311G(d,p) results were reasonable, the electronic structures of **VI** and **VII** (along with some other systems) were calculated at the B3LYP/6-311++G(d,p) (Table 2, data in parentheses) and at the B3LYP/6-311++G(2df,2p) (data not shown) levels, and the results of the B3LYP/6-311G(d,p) calculations were found to be consistent with the higher level calculations. (b) Sanz P, Yanez M, Mo O. *J. Phys. Chem. A* 2002; **106**: 4661 and references therein. (c) Minkin VI, Minyaev R. *Chem. Rev.* 2001; **101**: 1247 and references therein. (d) Schleyer PvonR, Maerker C, Dransfeld

- A, Jiao H, Hommes NJRvanE. *J. Am. Chem. Soc.* 1996; **118**: 6317.
86. A question can be raised as to whether the behavior observed for curves **a**, **c** and **d** is merely the influence of the subclass IB2 systems. To address this issue, an independent fitting was done using the data for only six systems of subclass IA1. The fitting gave the exponential curve labeled **b** as shown in the inset to Fig. 5. The regression function of curve **b** was then simply added to the main Fig. 5 to show the similarity of curve **b** to curves **a** and **c**. Curve **b** is thus obtained in the absence of the data for subclass IB2. Hence, the behavior observed for curves **a** and **c** is not due to the influence of the subclass IB2 systems. Alternatively, only subclass IA1 can be used for the  $E \leftrightarrow G$  correlation. But, as is evident from the plots, the final result would only be marginally different.
  87. In the work reported in references 23 and 24, two of the systems identified in this report to have intractable interactions were included. Hence, it is probably these two systems that led to the difference in behavior observed.
  88. As examples: for BAA, the derived  $E_{\text{HB,E}}$  (via eq. 2) is  $-18$  kcal/mol, as opposed to  $-16.3$  kcal/mol reported by Schiøtt *et al.*<sup>41</sup> Similarly, the derived  $E_{\text{HB,E}}$  for NMA is  $-28.9$  kcal/mol as opposed to the reported "HB energies" of about  $-27.1$  to  $-27.8$  kcal/mol.<sup>64</sup> The derived values in this work are again in good agreement with those reported.<sup>64</sup>
  89. Rosaz I, Alkorta I, Elguero J. *J. Phys. Chem. A* 2001; **105**: 10462.
  90. As in the case of the dependence of both  $H_b$  and  $E_{\text{HB,A}}$  on  $R(\text{O}\cdots\text{O})$  shown here, preliminary studies show that the dependence of  $V_b$  on  $R(\text{O}\cdots\text{O})$  is also exponential. Hence, the  $E_{\text{HB,A}}-V_b$  and  $E_{\text{HB,A}}-H_b$  correlation is not likely to be linear across all distances. The linear  $E_{\text{HB,A}}-V_b$  and  $E_{\text{HB,A}}-H_b$  correlation should therefore be interpreted as quasi-linear behavior.
  91. (a) These include the use of isodesmic reactions<sup>89</sup> and internal barrier energies.<sup>91b</sup> Korth *et al.*<sup>27</sup> have been attempted to use the former approach (as proposed by Rosa *et al.*<sup>89</sup>) to calculate IMHB enthalpies, but the attempt was not successful. Likewise, Grabowski<sup>75d</sup> has also pointed out that use of isodesmic reactions does not describe well the IMHB strength. The recently proposed approach to furnish HB energies from determination of barrier energies<sup>91b</sup> is not also expected to be successful (in addition to some cases for which it has been found not to be successful<sup>91b</sup>) when geometrical differences occur in the periphery of the H-bonded segment of a molecule as in the case of at least one system from class II (to be reported in a future communication). Hence, both of these approaches have not been pursued in this work. (b) Buemi G, Zuccarello F. *J. Mol. Struct. (Theochem)* 2002; **581**: 71–85.
  92. Chen JY-J, Naidoo KJ. *J. Phys. Chem. B* 2003; **107**: 9558–9566.
  93. (a) Humbel S. *J. Phys. Chem. A* 2002; **106**: 5517–5520 and references therein; (b) Pacios LF. *J. Phys. Chem. A* 2004; **108**: 1177–1188; (c) Smallwood CJ, McAllister MA. *J. Amer. Chem. Soc.* 1997; **119**: 11277–11281.
  94. Parthasarathi R, Subramanian V, Sathyamurthy N. *J. Phys. Chem. A* 2006; **110**: 3349–3351.
  95. Cremer D, Kraka E. *Croat. Chem. Acta.* 1984; **57**: 1259–1281.
  96. Bader RFW. *J. Phys. Chem. A* 1998; **102**: 7314–7323.
  97. (a) Jenkins S, Morrison I. *J. Chem. Phys. Lett.* 2000; **317**: 97–102; (b) Arnold WD, Oldfield E. *J. Am. Chem. Soc.* 2000; **122**: 12835–12841; (c) Espinosa E, Alkorta I, Elguero J, Molins E. *J. Chem. Phys.* 2002; **117**: 5529–5542.
  98. (a) Cremer D, Kraka E. *Angew. Chem.* 1984; **23**: 627; (b) Koch W, Frenking G, Gauss J, Cremer D, Collins JR. *J. Am. Chem. Soc.* 1987; **109**: 5917.
  99. The advantages the NBO approach can provide include: (a) It can partition the stereoelectronic interactions (SIs) into  $\pi$  and  $\sigma$  delocalization interactions thereby enabling the identification of the stabilizing and destabilizing ones upon H bonding. (b) Since there is a direct connection between NBO delocalization and resonance structures,<sup>100,101</sup> it should be a powerful tool for the study of resonance-assisted IMHBs—the NBO-based analysis may provide an important complementary advantage to the CSC analysis of the RAHB model in this regard. (c) It can provide "quantitative" information on the various D-A interactions, thus it is very suited for the comparative study of substituent-induced effects—such comparison is crucial for the rationalization of the relative strengths of IMHBs. (d) It can separate (and quantify) the D-A ability of the HB D-A interactions from all other interactions, hence the electronic bases of the inherent motion of the hydrogen atom due to H bonding may be modeled independently (at least indirectly).
  100. (a) Glendening ED, Weinhold F. *J. Comput. Chem.* 1998; **19**: 593; (b) Glendening ED, Weinhold F. *J. Comput. Chem.* 1998; **19**: 610; (c) Glendening ED, Badenshoop JK, Weinhold F. *J. Comput. Chem.* 1998; **19**: 628.
  101. Sproviero EM, Burton G. *J. Phys. Chem. A* 2003; **107**: 5544.
  102. (a) Rozas I, Alkorta I, Elguero J. *J. Phys. Chem. A* 1999; **103**: 8861; (b) Alkorta I, Elguero J, M6 O, Y6ñez M, Del Bene JE. *J. Phys. Chem. A* 2002; **106**: 9325; (c) Vorobyov I, Yappert MC, DuPr6 DB. *J. Phys. Chem. A* 2002; **106**: 668; (d) Klein RA. *J. Comput. Chem.* 2002; **23**: 587; (e) Green ME. *J. Phys. Chem. A* 2002; **106**: 11221; (f) Sosa GL, Peruchena NM, Contreras RH, Castro EAJ. *J. Mol. Struct. (Theochem)* 2002; **577**: 219; (g) Klein RA. *J. Am. Chem. Soc.* 2002; **124**: 13931; (h) Gonz6lez L, M6 O, Y6ñez M. *J. Phys. Chem. A* 1997; **101**: 9710, and references therein. (i) Marvi J, Grdadolnik J. *J. Phys. Chem. A* 2001; **105**: 2039.
  103. Reed AE, Weinstock RB, Weinhold FA. *J. Chem. Phys.* 1985; **83**: 735, and references in ref. 99d. In comparison with the Mulliken population analysis, the natural population analysis (NPA) is known to be more stable with the size of basis functions used.
  104. (a) Reed AE, Weinhold F. *J. Chem. Phys.* 1985; **83**: 1736; (b) Reed AE, Weinhold F. *J. Chem. Phys.* 1983; **78**: 4066; (c) Reed AE, Weinhold F, Curtiss LA, Pochatko DJ. *J. Chem. Phys.* 1986; **84**: 5687.
  105. The systems we are investigating are inherently highly delocalized. As pointed out recently by Alabugin *et al.*,<sup>105b</sup> when a system is intrinsically highly delocalized, the NBO analysis, which is based on a single dominant structure, yields a qualitative description of the system with contributions from other resonance structures treated as the second-order perturbation corrections. In view of this, our analysis is "quantitative" only in a relative sense since we are comparing different systems that are structurally related to a prototype system. In this regard, our prototype system is the MAE molecule, and in some cases both MAE and AAE are used since both of are well-understood systems. (b) Alabugin IV, Monoharan M, Weinhold FA. *J. Phys. Chem. A* 2004; **108**: 4720–4730.
  106. For example, the HB interaction energy has been shown by NBO analysis at the B3LYP/6-311++G(d,p) level to correlate with the second-order interaction energies and the charge transferred.<sup>102a,b</sup> There are also several other reports that showed the NBO method can be used successfully to investigate substituent-induced effects.<sup>107–109</sup> Alem *et al.*<sup>109a</sup> have also shown NBO charge calculated by the B3LYP and the post-HF methods to be in good agreement with each other and generally display only a marginal basis-set dependence—consistent with previous findings which showed that NBO charges are only slightly affected by basis set variations and consequently are better suited to analyze the electronic properties.<sup>109b,c</sup>
  107. (a) Alabugin IV, Manoharan M, Peabody S, Weinhold F. *J. Am. Chem. Soc.* 2003; **125**: 5973, and references therein; (b) Alabugin IV, Zeidan TA. *J. Am. Chem. Soc.* 2002; **124**: 3175.
  108. Wong NB, Cheung YS, Wu DY, Ren Y, Tian AM, Li WK. *J. Phys. Chem. A* 2000; **104**: 6077.
  109. (a) Alem Kv, Sudh6lter EJR, Zuilhof H. *J. Phys. Chem. A* 1998; **102**: 10860–10868. The Alem *et al.* study is consistent with previous findings that showed that NBO charges are only slightly affected by basis set variations;<sup>109b,c</sup> (b) Bachrach SM. In *Reviews in Computational Chemistry*, Lipowitz KB, Boyd DB (eds). VHC Publishers: New York; pp 379–390; (c) Wiberg KB, Rablem PR. *J. Comput. Chem.* 1993; **14**: 1504–1518; (d) Sosa GL, Peruchena NM, Contreras RH, Castro EA. *J. Mol. Struct.* 2002; **577**: 219–228; (e) Parreira RLT, Galembeck SE. *J. Am. Chem. Soc.* 2003; **125**: 15614; (f) Green ME. *J. Phys. Chem. A* 2004; **108**: 6543–6553.
  110. Even though the  $E(2)_{\text{O2}}$  data (Tables 5 and 6) have been obtained at the B3LYP/6-311++G(d,p) level, the  $E_{\text{HSE}}$  and  $E_{\text{HBE}}$  data at the B3LYP/6-311G(d,p) level are used here because it has already been shown that there is no significant difference (within the 1–2 kcal/mol limits of experimental error) in the HB stabilization energies ( $E_{\text{HSE}}$ 's) calculated at the two levels of theory.